PLOS ONE

RESEARCH ARTICLE

Application of machine learning and complex network measures to an EEG dataset from ayahuasca experiments

Caroline L. Alves[1,2]*, **Rubens Gisbert Cury**[3], **Kirstin Roster**[2], **Aruane M. Pineda**[2], **Francisco A. Rodrigues**[2], **Christiane Thielemann**[1], **Manuel Ciba**[1]

1 BioMEMS Lab, Aschaffenburg University of Applied Sciences (UAS), Aschaffenburg, Germany, **2** Institute of Mathematical and Computer Sciences, University of São Paulo (USP), São Paulo, Brazil, **3** Department of Neurology, Movement Disorders Center, University of São Paulo (USP), São Paulo, Brazil

* Caroline.Alves@th-ab.de

Citation: Alves CL, Cury RG, Roster K, Pineda AM, Rodrigues FA, Thielemann C, et al. (2022) Application of machine learning and complex network measures to an EEG dataset from ayahuasca experiments. PLoS ONE 17(12): e0277257. https://doi.org/10.1371/journal.pone.0277257

Editor: Yiming Tang, Hefei University of Technology, CHINA

Received: August 1, 2022

Accepted: October 23, 2022

Published: December 16, 2022

Peer Review History: PLOS recognizes the benefits of transparency in the peer review process; therefore, we enable the publication of all of the content of peer review and author responses alongside final, published articles. The editorial history of this article is available here: https://doi.org/10.1371/journal.pone.0277257

Data Availability Statement: The data used in this work may be obtained here: Ekman Schenberg, Eduardo, 2015, "Acute Biphasic effects of

Abstract

Ayahuasca is a blend of Amazonian plants that has been used for traditional medicine by the inhabitants of this region for hundreds of years. Furthermore, this plant has been demonstrated to be a viable therapy for a variety of neurological and mental diseases. EEG experiments have found specific brain regions that changed significantly due to ayahuasca. Here, we used an EEG dataset to investigate the ability to automatically detect changes in brain activity using machine learning and complex networks. Machine learning was applied at three different levels of data abstraction: (A) the raw EEG time series, (B) the correlation of the EEG time series, and (C) the complex network measures calculated from (B). Further, at the abstraction level of (C), we developed new measures of complex networks relating to community detection. As a result, the machine learning method was able to automatically detect changes in brain activity, with case (B) showing the highest accuracy (92%), followed by (A) (88%) and (C) (83%), indicating that connectivity changes between brain regions are more important for the detection of ayahuasca. The most activated areas were the frontal and temporal lobe, which is consistent with the literature. F3 and PO4 were the most important brain connections, a significant new discovery for psychedelic literature. This connection may point to a cognitive process akin to face recognition in individuals during ayahuasca-mediated visual hallucinations. Furthermore, closeness centrality and assortativity were the most important complex network measures. These two measures are also associated with diseases such as Alzheimer's disease, indicating a possible therapeutic mechanism. Moreover, the new measures were crucial to the predictive model and suggested larger brain communities associated with the use of ayahuasca. This suggests that the dissemination of information in functional brain networks is slower when this drug is present. Overall, our methodology was able to automatically detect changes in brain activity during ayahuasca consumption and interpret how these psychedelics alter brain networks, as well as provide insights into their mechanisms of action.

ayahuasca", https://doi.org/10.7910/DVN/VVE6QC, Harvard Dataverse, V1 This information may be found here: Schenberg EE, Alexandre JFM, Filev R, Cravo AM, Sato JR, Muthukumaraswamy SD, et al. (2015) Acute Biphasic Effects of Ayahuasca. PLoS ONE 10(9): e0137202. https://doi.org/10.1371/journal.pone.0137202 doi: 10.1371/journal.pone.0137202 We also uploaded the Pearson connectivity matrix from the original data in the following Figshare repositories here: Pearson's connection matrix of the EEG experiments of subjects who ingested Ayahuasca at the time after the psychedelic activation time can be found here: Alves, Caroline (2022): With-ayahuasca. Figshare repository. Dataset. https://doi.org/10.6084/m9.figshare.21082513.v1 Pearson's connection matrix of the EEG experiments of subjects who ingested Ayahuasca at the time before the psychedelic activation time: Alves, Caroline (2022): No-ayahuasca. Figshare repository. Dataset. https://doi.org/10.6084/m9.figshare.21082531.v1.

Funding: This study was financially supported by Conselho Nacional de Desenvolvimento Científico e Tecnológico (CNPq) in the form of a grant awarded to FAR (309266/2019-0). This study was also financially supported by Fundação de Amparo à Pesquisa do Estado de São Paulo (FAPESP) in the form of grants awarded to FAR (19/23293-0), AMP (2019/22277-0) and KR (2019/26595-7). The funders had no role in study design, data collection and analysis, decision to publish, or manuscript preparation.

Competing interests: The authors have declared that no competing interests exist.

1 Introduction

Ayahuasca is made from a blend of Amazonian herbs [1]. This combination of plants is often associated with rituals of different religions and social groups. Ayahuasca has been used in the Amazon for a couple of hundred years, being part of the traditional medicine of the indigenous population within this region [2].

Since the use of ayahuasca has spread throughout many countries, it is necessary to study in depth its cerebral mechanisms and its potential clinical implications. In addition, because it affects brain areas related to emotions, memories, and executive functions, ayahuasca might be used in the treatment of psychiatric disorders, such as drug addiction [3–5], Parkinson's disease [6–9], and depression [10–16]. For example, an open-label clinical study found significant therapeutic benefits among patients with treatment-resistant major depressive disorder after the administration of a single dose of ayahuasca [12]. Moreover, a randomized trial showed that ayahuasca doses were associated with reductions in depressive symptoms in patients with major depressive disorder, compared to placebo treatments [11].

Additionally, ayahuasca has been shown to elicit anti-neuroinflammatory properties [16] and stimulate adult neurogenesis in vitro [17]. In this line, ayahuasca could be helpful for the treatment of several neurological diseases well known to harbor inflammation in its physiopathology [18], including chronic degenerative diseases and illnesses related to acute injury, such as cerebral ischemia, multiple sclerosis, and Alzheimer's disease (AD) [19, 20].

The EEG data studied here are from [21], from subjects who ingested ayahuasca. This study observed slow-gamma power increases at the left Centro-parietal-occipital, left frontotemporal, and right frontal cortices. In contrast, fast-gamma increases were significant at the left Centro-parieto-occipital, left frontotemporal, right frontal, and right parieto-occipital cortices due to ayahuasca ingestion. As a result, this study concentrated solely on the changes in frequency bands caused by the use of the psychedelic substance.

Despite the enormous therapeutic potential of ayahuasca, in most countries, it is an illegal substance and only legalized for religious use, such as in Brazil. Therefore, few studies on human beings are found in the literature, and more research is needed on how this substance alters the brain and its mechanism of action.

The use of graph theory mathematical approaches gave intriguing insights into the intricate network structure of the human brain, which is also related with pathological states [22–25]. Notably, complex networks have been employed as biomarkers for a variety of disorders [26, 27]. Furthermore, the community detection algorithm (also referred to as the clustering graph) is a fundamental analysis technique that aims to identify densely connected structures within complex networks [28–30]. Several studies have used complex network measurements and community detection algorithms to detect brain activity in EEG data recently [31–33]

Because of the increased amount of data related to health, such as medical records, exams of patients, and hospital resources, machine learning (ML) algorithms have become more applicable, primarily for medical diagnosis [34–37], in order to provide more accurate and automatic investigations of various diseases [38] and may be an important tool capable of detecting acute and permanent abnormalities in the brain. In addition, many studies have utilized machine learning algorithms to capture brain activity using raw EEG time series [39, 40], the correlation between electrodes [41, 42], and complex network measures [23].

Also, in contrast to traditional statistical methods, the ML approach has the advantage that it does not rely on prior assumptions (such as adequate distribution, independence of observations, absence of multicollinearity, and interaction problems) and is also well suited to analyze and capture complex nonlinear relationships in data automatically. Nevertheless, new techniques have emerged to assist in interpreting machine learning results, e.g., SHapley Additive

Explanations (SHAP) values. Any machine learning algorithm may use this metric for identifying and prioritizing features [43–45].

The purpose of this study is to determine whether it is possible to automatically detect the changes in brain activity after intake of ayahuasca with machine learning methods using the following data abstraction levels for the input: (A) raw EEG time series, (B) the correlation between the EEG electrodes as used in (A) represented by a connectivity matrix, and (C) complex network measures extracted from (B). In contrast to articles in the literature that use only one of these levels of abstraction, this study uses all three levels. In addition, we define which of these abstraction levels is most appropriate for capturing ayahuasca-induced brain changes. The SHAP value method has also been shown to be more effective than the studies cited above in identifying the best brain regions, the best connections between the brain regions, and the best measures of complex networks, which can be used to interpret the effects of the psychedelic substance on the brain. A final result of this research was the creation of new measures that have never been used before within the literature, which can be used as input to machine learning algorithms to assess the size of community structures.

2 Materials and methods

The python code used for the analysis is available at https://github.com/Carol180619/Paper-ayahuasca.git.

2.1 Data

The data used for this study has been made openly available by the Federal University of São Carlos, Brazil [21]. Sixteen healthy male and female patients with prior ayahuasca experience (eight women, mean 29.0 years; 12 men, mean 38.5 years) agreed (with written permission) to consume this psychedelic substance while EEG recordings were made (The following exclusion criteria were used: minors than the age of 21 years, personal history of psychiatric illness, current use of any psychiatric medication, cardiovascular disease, and any neurological disorders or brain damage in the previous year). All methodologies for this investigation were approved by the Universidade Federal de São Paulo's Ethical Committee, and the study was carried out in compliance with available criteria for human hallucinogen research safety [46].

Patients were instructed to close their eyes and remain in a resting condition. A nurse accompanied the experiment for its duration of 225 minutes. The recordings began 25 minutes before ayahuasca consumption and ended 200 minutes afterward. The main compounds in the brew were [21]: Dimethyltryptamine (DMT), DMTN-oxide (DMT-NO), N-methyltryptamine (NMT), indoleacetic acid (IAA), 5-hydroxy-DMT (5-OH-DMT, or bufotenin), 5-methoxy-DMT (5-MeO-DMT), Harmine, Harmol, Harmaline, Harmalol, THH, 7-hydroxy-tetrahydroharmine (THH-OH), and 2-methyl-tetrahydro-beta- carboline (2-MTHBC). All recordings were downsampled to 500 Hz, bandpass filtered between 0.5 and 150 Hz, and artifacts due to movements were removed. Recordings were made with 62 electrodes, following the EEG electrode positions in the 10–10 system. These channels are: Fp1, Fz, F3, F7, FT9, FC5, FC1, C3, TP9, CP5, CP1, Pz, P3, P7, O1, Oz, P8, TP10, CP6, CP2, C4, T8, FT10, FC6, FC2, F4, F8, Fp2, AF7, AF3, AFz, F1, F5, FT7, FC3, FCz, C1, C5, TP7, CP3, P1, P5, PO7, PO3, POz, PO4, PO8, P6, P2, CPz, CP4, TP8, FC4, FT8, F6, F2, AF4, AF8, O2, P4, C6, and C2 (see in Appendix A (Fig 13) of S1 Appendix). It is worth mentioning that after using ayahuasca, all individuals experienced notable alterations in their typical state of consciousness.

Further details are given in [21].

2.2 Machine learning algorithm

2.2.1 Classification. In order to classify the (A) EEG time series, (B) the connectivity matrices, and (C) the complex network measures, the support vector machine (SVM) [47] algorithm was used. SVM has been used with superior results for the classification of complex network measures before by other groups [48–50] and performed superior in our comparative evaluation. In this analysis, we compared the following machine learning methods to classify the complex network measures: Random forest (RF) [51], SVM [47], naive bayes (NB) [52], multilayer perceptron (MLP) [53], stochastic gradient descent with linear models classifier (SGD) [54], logistic regression (LR) [55] and extreme Gradient Boosting classifier [56] (XGBoost). The results can be found in Appendix C in S1 Appendix.

A more robust deep learning (DL) algorithm from [41] (in which the model was named tuned convolutional neural network) was also tested. The results using DL are in the Appendix D in S1 Appendix.

2.2.2 Resampling and evaluation. The dataset was resampled by separating it into training (train) and test sets, with 25% of data composing the test set. Then, for a reliable model, a k-cross validation was used [57], with k = 10 (value widely used in the literature [58–62]). A hyper-parameter optimization called grid search was used here, similar to [63–67]. The hyper-parameter optimization values used for each classifier models can be found in Appendix C in S1 Appendix.

For evaluation, accuracy (Acc.) was used as the standard performance metrics, as is the state-of-art in the literature [37, 68–71]. Since the problem here is a two-class (negative and positive) classification problem, other metrics considered here are the measures of precision and recall, also commonly used in the literature [72–75]. Precision (also called positive predictive value) is the proportion of relevant instances among those retrieved. Whereas recall (also called sensitivity) measures how well a classifier can predict positive examples (hit rate in the positive class), here related with an effect of the ayahuasca. Another measure used here and also used in literature [64, 76, 77] is the F1 score which is the harmonic mean of the recall and precision [78]. For visualization of these two latter measures, the receiver operating characteristic (ROC) curve is a standard method as it displays the relation between the rate of true positives and false positives. The area below this curve, called the area under the ROC curve (AUC), has been widely used in classification problems [66, 68, 79, 80]. The value of the AUC varies from 0 to 1, where the value of one corresponds to a classification result free of errors. $AUC = 0.5$ indicates that the classifier is not able to distinguish the two classes; this result is equal to the random choice. Furthermore, we consider the micro average of the ROC curve, which computes the AUC metric independently for each class (calculate AUC metric for healthy individuals, class zero, and separately calculate for unhealthy subjects, class one), and then the average is computed considering these classes equally. The macro average is also used in our evaluation, which does not consider both classes equally, but aggregates the contributions of the classes separately and then calculates the average.

Furthermore, we interpret the machine learning results using SHapley Additive exPlanations (SHAP) values [81] to quantify the importance of the complex measures, connections of brain regions, and location of electrodes for the classification result. This metric enables the identification and prioritization of features and can be used with any machine learning algorithm [43–45].

2.3 Input data for machine learning

The following three data abstraction levels were applied to a classification algorithm as described in subsection 2.2 Machine learning algorithm: (2.3.1 EEG time series) the EEG time

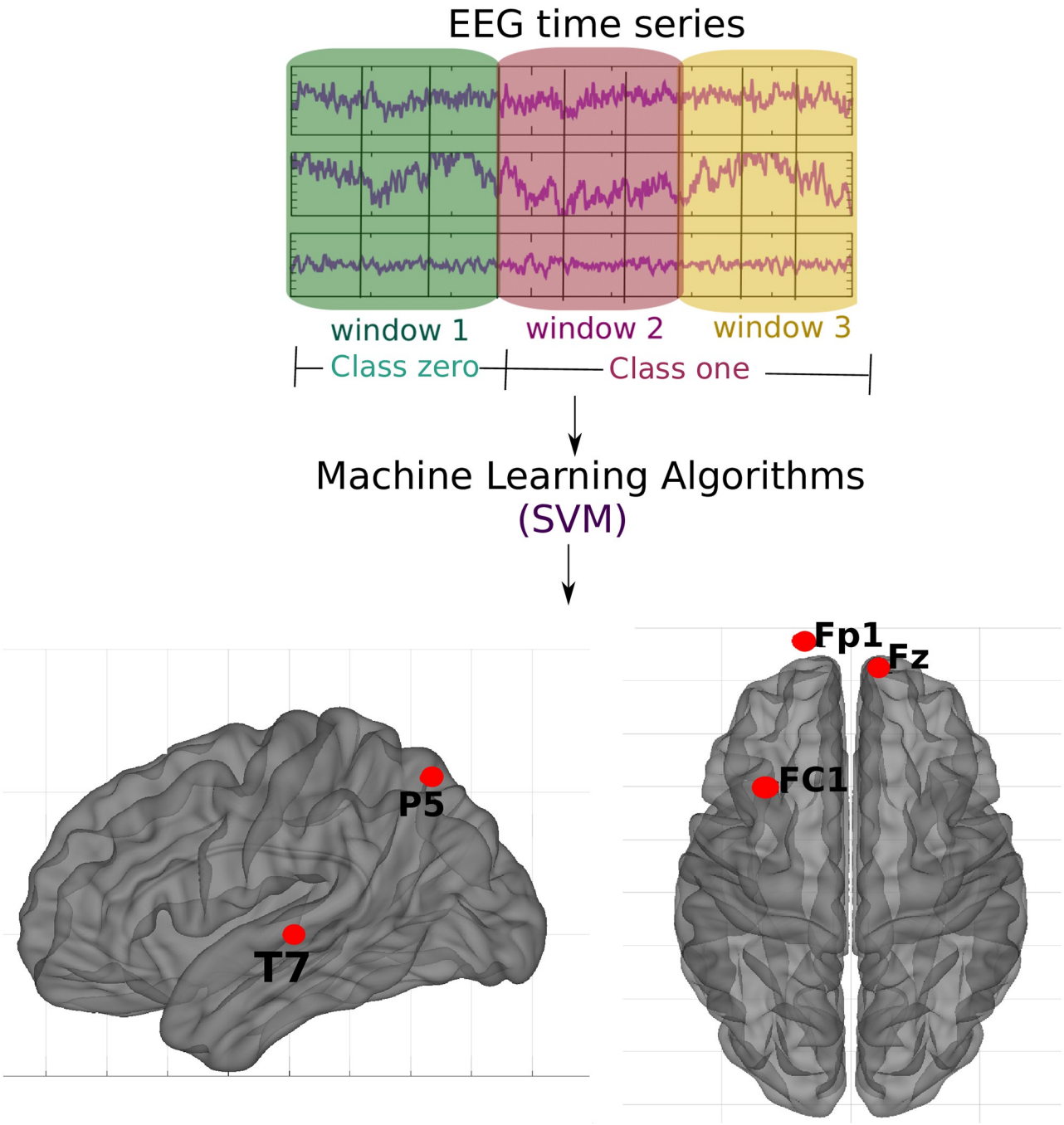

Fig 1. Methodology of the subsection using raw EEG time series. For each participant, the EEG time series was split into three parts. Those corresponding to the first window were labeled as class 0 (no effect of ayahuasca) and those corresponding to the second and third windows as class 1 (under the influence of ayahuasca), and then SVM was used. The objective was to determine which brain parts are most influenced by ayahuasca consumption. The crucial areas discovered using the SHAP values approach are emphasized in the illustration.

https://doi.org/10.1371/journal.pone.0277257.g001

series (Fig 1), (2.3.2 Connectivity matrices) the connectivity matrix calculated by means of the Pearson correlation of the EEG time series (Fig 2), and (2.3.3 Complex network measures) the complex network measures calculated from the connectivity matrix (Fig 3).

2.3.1 EEG time series. The data was divided into three "time windows" (see Table 1). The first window (25 minutes before ingestion until 50 minutes after ingestion of ayahuasca) was

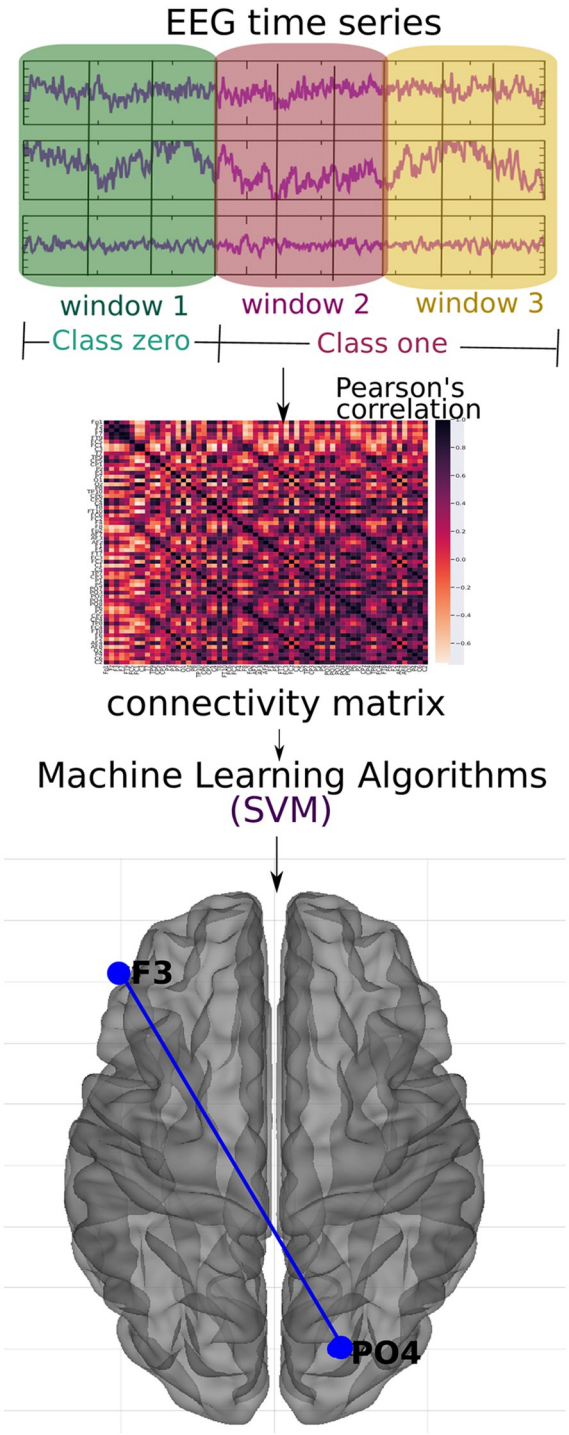

Fig 2. Methodology of the subsection using connectivity matrices. For each of the time windows, the Pearson correlation connectivity matrix was generated, and then they were classified with the SVM method considering the first window as zero label (without ayahuasca) and the other two as one label (with ayahuasca). This analysis aimed to verify the best connections of the brain areas used during ayahuasca use. The principal connection discovered using the SHAP value approach is depicted in the picture.

https://doi.org/10.1371/journal.pone.0277257.g002

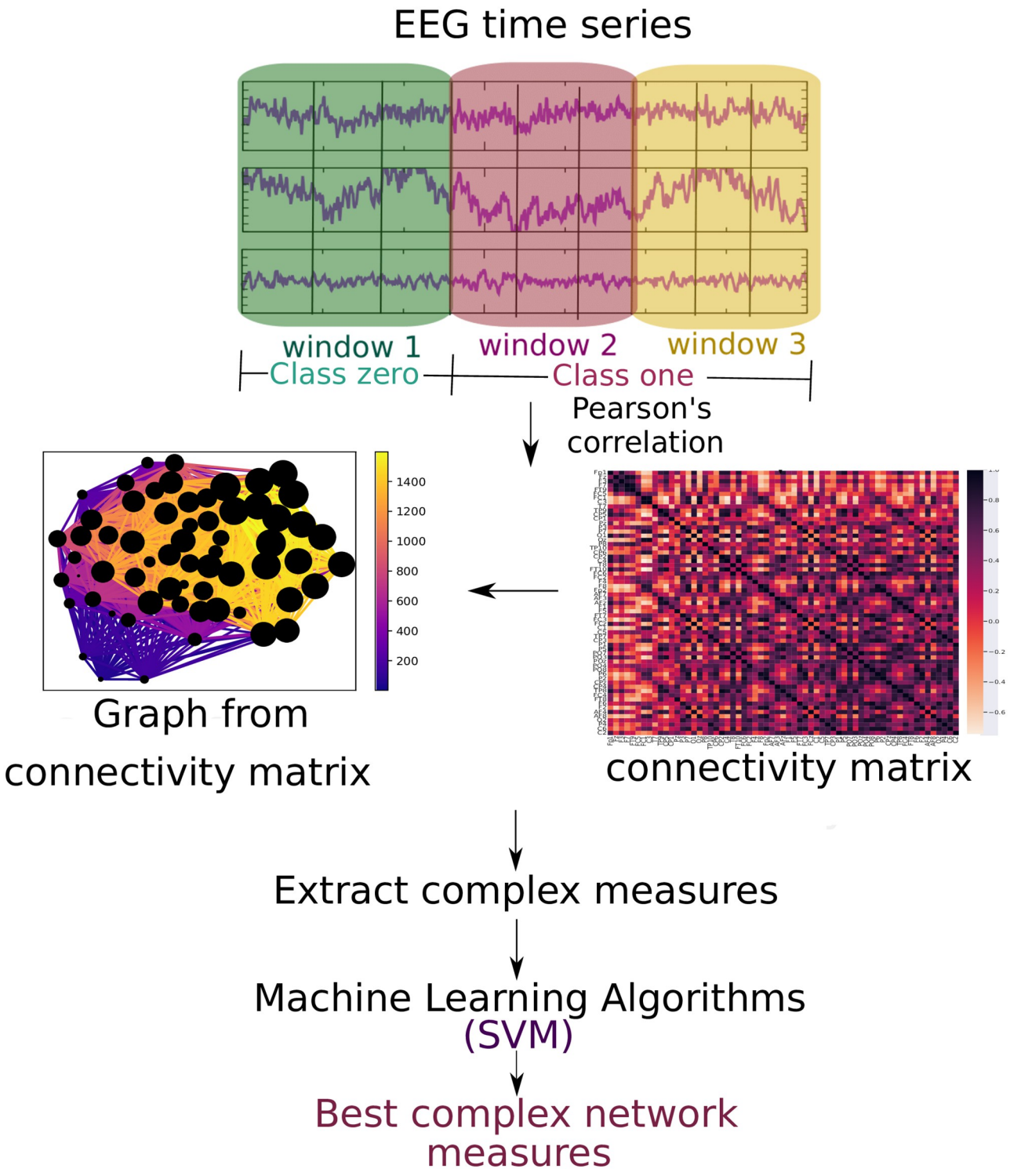

Fig 3. Methodology of the subsection using complex network measures. The EEG time series is divided into three parts. For each of them, the Pearson correlation was calculated. For each window, a connectivity matrix was generated (in the Fig, the connectivity matrix of the first window of the first subject containing the 62 electrodes, the color bar containing the connection strength between these electrodes). A graph was formed for each of them (in the Fig, the graph of this connectivity matrix has 62 nodes and the connection strength according to the color bar and the node size according to its number of connections), and complex network measures are extracted from them.

https://doi.org/10.1371/journal.pone.0277257.g003

Table 1. Definition of time windows of the EEG signal. Window 1 is considered the control (without effect of ayahuasca), window 2 and 3 are considered as recordings under the influence of ayahuasca.

Time window	Ingestion of ayahuasca at t = 0 minutes
1	-25 to 50 minutes
2	50 to 125 minutes
3	125 to 200 minutes

https://doi.org/10.1371/journal.pone.0277257.t001

defined as the "control". This is reasonable as it is known from [21], that the blood plasma concentration of the main psychedelic compound DMT is low until 50 minutes after ingestion. Windows two and three were both defined as thoroughly influenced by ayahuasca. The ayahuasca-influenced time series were divided into two windows to enhance the quantity of data points for the machine learning method. Even though the number of independent samples (subjects) did not change, increasing the data points by splitting the time series is a common machine learning approach [82, 83]. Even though the number of independent samples (subjects) did not change, increasing the data points by splitting the time series is a standard machine learning approach. Furthermore, in the following classification task, only two classes will be labeled class zero (without ayahuasca) and labeled class one (with ayahuasca). The scheme of this methodology is shown in Fig 1. All participants' EEG time series were successively combined and stored in a 2D matrix to feed the data into the machine learning algorithm. Each column represents an electrode, and each row represents the amplitude of each time point of the EEG signal. For each of the three time windows, a 2D matrix was constructed.

2.3.2 Connectivity matrices. The matrices of connectivity were calculated by the well known Pearson correlation. It is a widely used and successfully approved measure to capture the correlation of EEG electrodes [84–88].

The Pearson correlation was calculated for all electrode pairs resulting in three connectivity matrices per participant (for each time window). Fig 2 illustrates the workflow of this approach. The connectivity matrices were flattened into one vector to input the data into the machine learning algorithm. Then, all vectors were sequentially merged into a 2D matrix. Each column represents a connection between two brain regions, and each row represents a subject. Such a 2D matrix was generated for each of the three time windows.

2.3.3 Complex network measures. For each connectivity matrix (see subsection 2.3.2 Connectivity matrices), a graph was generated to extract different complex network measures. The complex network measures were stored in a matrix to input the data into the machine learning algorithm. Each column represents a complex network measure, and each row a subject. Such a 2D matrix was generated for each of the three time windows. The following complex network measures were calculated: Assortativity [89, 90], average path length (APL) [91], betweenness centrality (BC) [92], closeness centrality (CC) [93], eigenvector centrality (EC) [94], diameter [95], hub score [96], average degree of nearest neighbors [97] (Knn), mean degree [98], second moment degree (SMD) [99], entropy degree [100], transitivity [101, 102], complexity, k-core [103, 104], eccentricity [105], density [106], and efficiency [107]. Furthermore, newly developed metrics reflecting the number of communities in a complex network are used in this paper.

Furthermore, newly developed metrics reflecting the number of communities in a complex network are used in this paper. We perform the community detection algorithms to find the largest community, then calculate the average path length within this community and receive a single value as a result (that will be used to feed ML algorithm). The community detection algorithms used were:

- Fastgreedy community (FC) is defined in [108] as a hierarchical agglomerative clustering algorithm aimed at maximizing the modularity measure defined in [109].
- Infomap community (IC) Infomap community (IC) described in [110], the purpose behind this technique is to exploit the dynamics of random walks. This is accomplished by employing Huffman's method [111] and then calculating the minimization of the map equation to determine the number of communities [110].
- Leading eigenvector community (LC) is defined in [112]. It aims to calculate the eigenvector of the modularity matrix for the largest positive eigenvalue and then separate the vertices into two communities based on the sign of the corresponding element in the eigenvector.
- Label propagation community (LPC) is defined in [113]. It is an optimization algorithm [114] in which, at first, each node in the network has a label indicating its assignment, and then each node updates its label according to the label with the maximum number in its neighbors. This process is repeated until the network reaches a stable state and nodes with the same class are considered to belong to the same community. [115].
- Edge betweenness community (EBC) is defined in [109] is a divisive model based on the BC. At each iteration, this measure is calculated for all edges, and the one with the highest value of this measure is eliminated until the network contains N elements resulting in a hierarchical distribution of communities. The one with the highest modularity is adopted.
- Spinglass (SPC) is defined in [116] this algorithm considers the spin state of nodes as communities and tries to minimize the spin energy until it finds a ground state of the spin-glass model [117].
- Multilevel community (ML) Multilevel community (ML) is a greedy optimization method using modularity and is defined in [118].

Since the community detection algorithms were combined with the average path length, we extended the abbreviations by the letter "A" as follows: AFC, AIC, ALC, ALPC, AEBC, ASPC, and AMC.

Fig 3 depicts the entire workflow.

3 Results

The highest classification performance was obtained using the connectivity matrices with an accuracy of 92%, followed by the EEG time series (88%) and the complex network measures (83%) (see Table 2). The following subsections 3.1 EEG time series, 3.2 Connectivity matrices and 3.3 Complex network measures contain the results in more detail.

Table 2. Performances of the SVM classifier for the different data types used in this paper. The best performance is highlighted in bold. The classification of connectivity matrices best captured the changes in the brain due to ayahuasca.

Type of data	Subset	AUC	Acc.	F1 score	Recall	Precision
EEG time series	**Train**	0.87	0.89	0.88	0.87	0.89
	Test	0.85	0.88	0.86	0.85	0.86
Connectivity matrix	**Train**	**0.92**	**0.94**	**0.93**	**0.92**	**0.96**
	Test	**0.88**	**0.92**	**0.90**	**0.88**	**0.94**
Complex measure	**Train**	0.79	0.81	0.79	0.79	0.78
	Test	0.75	0.83	0.78	0.75	0.90

https://doi.org/10.1371/journal.pone.0277257.t002

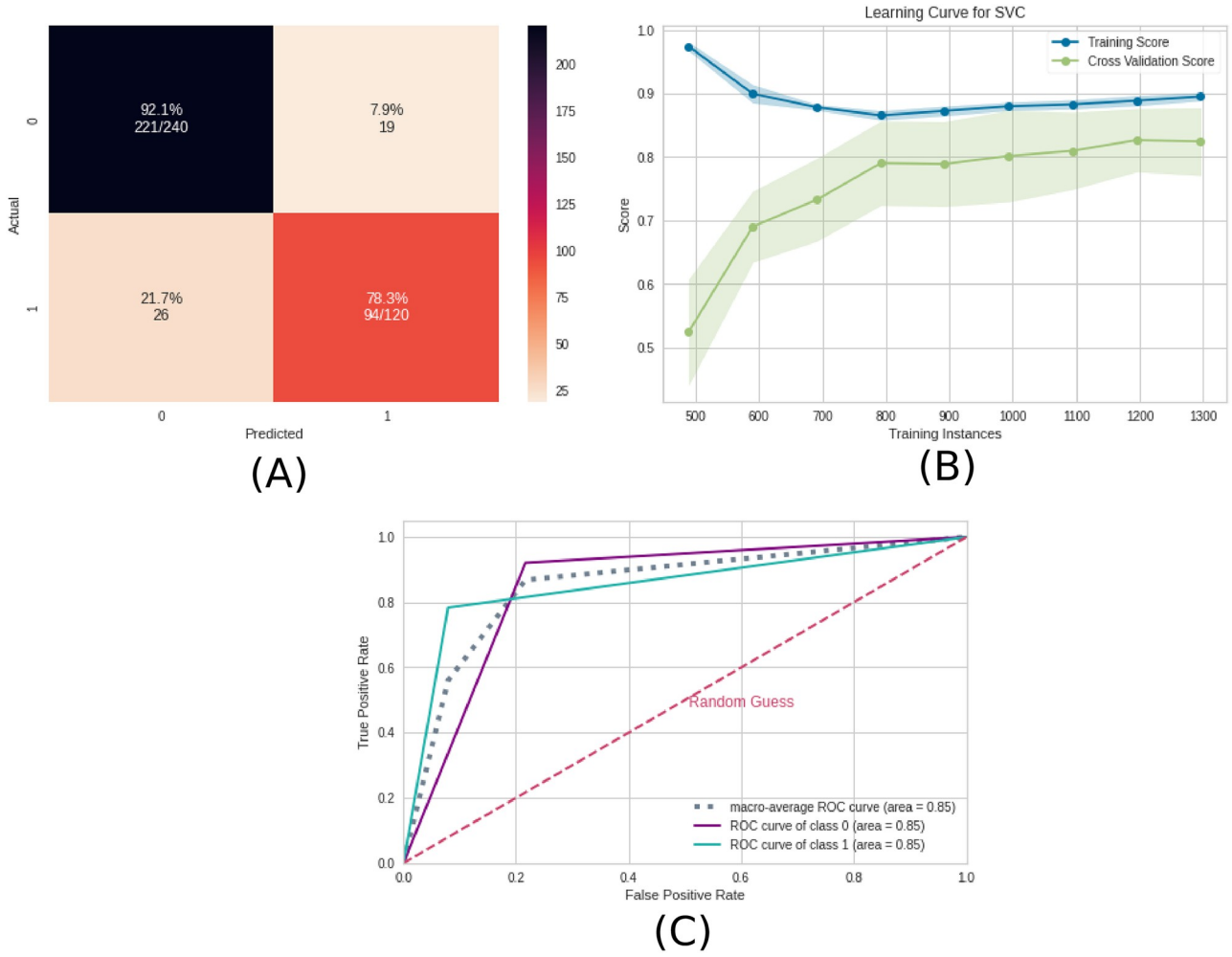

Fig 4. Machine learning results using the EEG time series as input data. A) Confusion matrix indicating a true negative rate of 92.1% (blue according to the color bar) and a true positive rate of 78.3% (orange according to the color bar). B) Learning curve for the training accuracy (blue) and for test accuracy (green). C) ROC curve of class 0 (without ayahuasca) and class 1 (with ayahuasca). The gray dotted curve is the macro-average accuracy (area under curve = 0.85) and the pink one the random classifier.

https://doi.org/10.1371/journal.pone.0277257.g004

3.1 EEG time series

The performance of the test sample using the EEG time series was mean AUC of 0.85, mean precision of 0.88, mean F1 score of 0.86, mean recall of 0.85, and mean accuracy of 0.86. The precision measure is related to the positive class (with ayahuasca). Since the precision measure was slightly higher than the recall measure, the model can better detect the presence of ayahuasca instead of the absence of it.

In Fig 4, the confusion matrix (Fig 4A), the learning curve (Fig 4B), and the ROC curve (Fig 4C) are plotted.

The learning curve evaluates the predictability of the model by varying the size of the training set [45]. Fig 4B shows that the highest accuracy in the test sample can only be achieved when the entire database is used.

Not all electrodes of the EEG recording were equally important for the classification. According to the SHAP values, the most important region for the model was T7, located in the temporal region (see Fig 5). In order of importance, this region was followed by FC1, Fp1, P5,

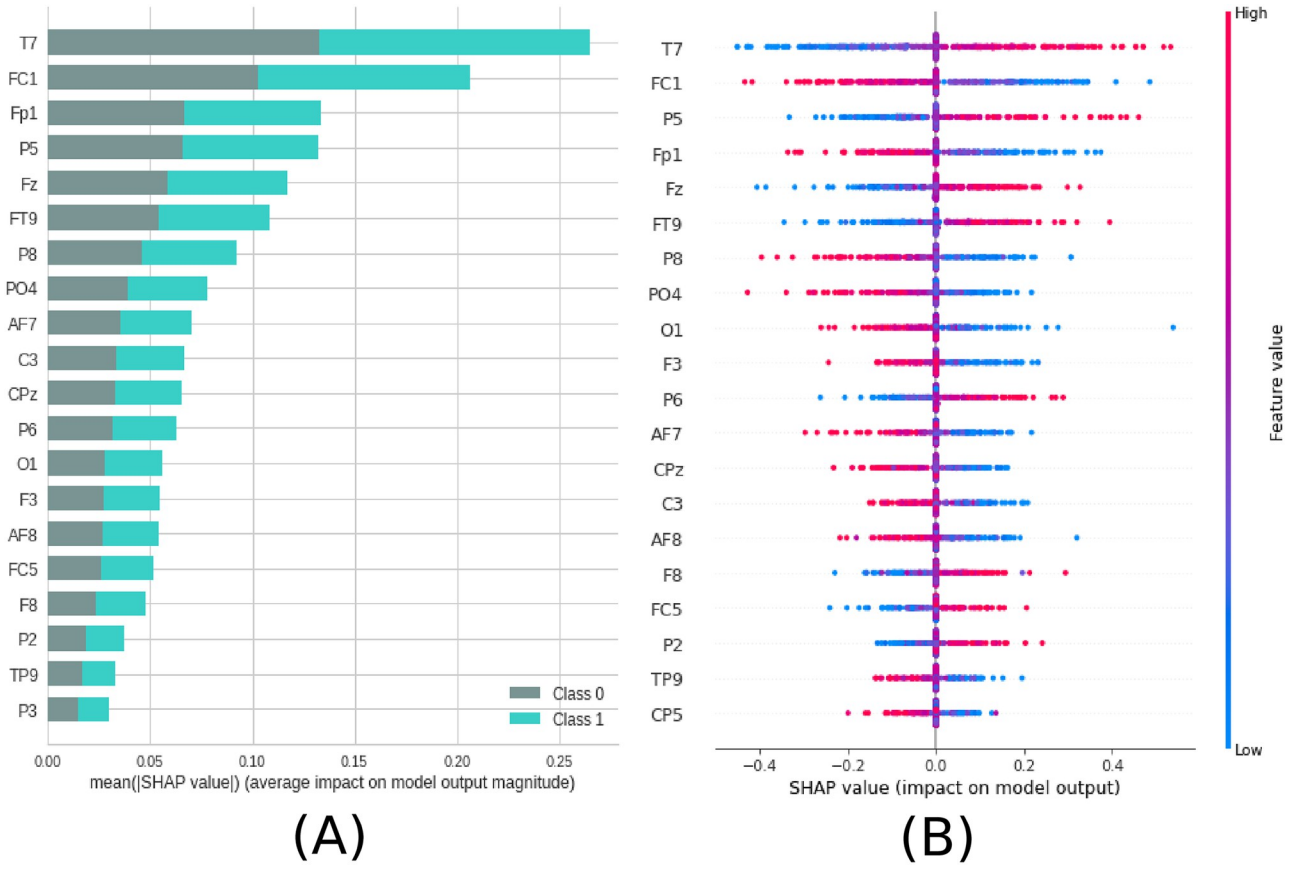

Fig 5. Feature importance ranking for SVM classifier being the brain regions ranked in descending order of importance. Brain region T7 is most important to classify the effect of ayahuasca. A) Feature ranking based on the average of absolute SHAP values over all subjects considering both classes (gray:without ayahuasca, cyan: with ayahuasca). B) Same as A) but additionally showing details of the impact of each feature on the model.

https://doi.org/10.1371/journal.pone.0277257.g005

and Fz, located between frontal and central, frontal and parietal, parietal and frontal, respectively (see Fig 6A). In addition, Fig 6B shows details of the impact of each feature on the model. Positive SHAP values are shown when the presence of ayahuasca is detected, and negative SHAP values are shown when the absence of ayahuasca is detected. The colors indicate whether the feature value was low (blue) or high (red). Since the feature consists of the amplitudes of the EEG time series, it can be seen that for T7, the low amplitudes (blue dots) were important to detect the absence of ayahuasca (negative SHAP values), and the high amplitudes (red dots) were important to detect the presence of ayahuasca (positive SHAP values).

3.2 Connectivity matrices

For the connectivity matrices, the test sample performance was a mean AUC of 0.88, mean accuracy of 0.92, mean F1 score of 0.90, mean recall of 0.88, and mean precision of 0.94.

Similar to the previous subsection 3.1 EEG time series, the precision measure was higher than the recall measure and therefore the model can better detect the presence of ayahuasca. In Fig 7, the confusion matrix (Fig 7A), the learning curve (Fig 7B), and the ROC curve (Fig 7C) are plotted. Similar to EEG time series, the learning curve for the connectivity matrices shows that the highest accuracy in the test sample can only be achieved when the entire database is used.

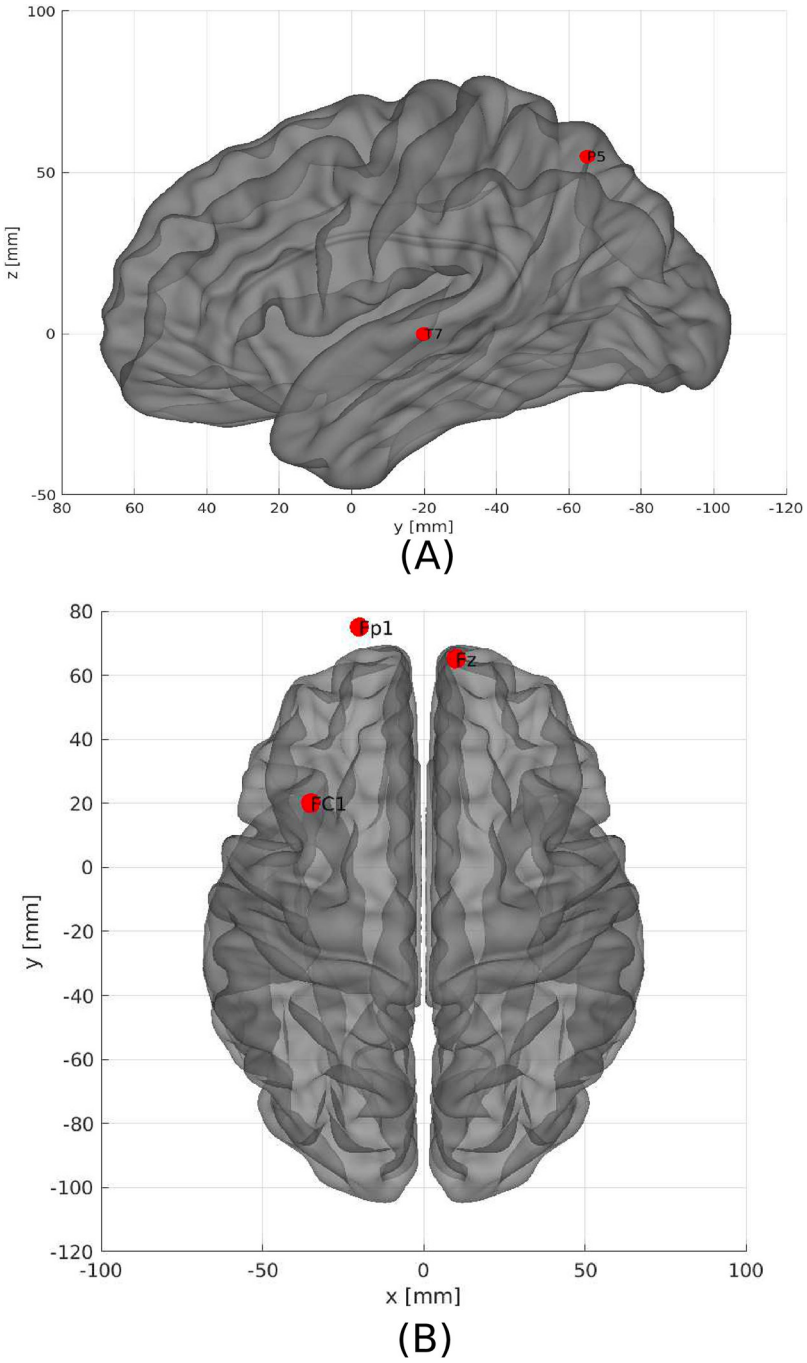

Fig 6. The five most important brain regions considering EEG time series as input data. A)—Sagittal left plane showing the brain region for the channel T7 and P5. B) Axial dorsal plane showing the brain regions Fz, Fp1 and FC1. The brain plot was made using Braph tool [119], based on the coordinates in [120, 121].

https://doi.org/10.1371/journal.pone.0277257.g006

In order to reveal the importance of the brain connections, the SHAP values were used as in the preview subsection 3.1 EEG time series. The results are shown in Fig 8. From that the most important connection was between F3 (frontal region) and PO4 (between parietal and occipital region). In addition, in Fig 8B it can be seen that for the connection between F3 and

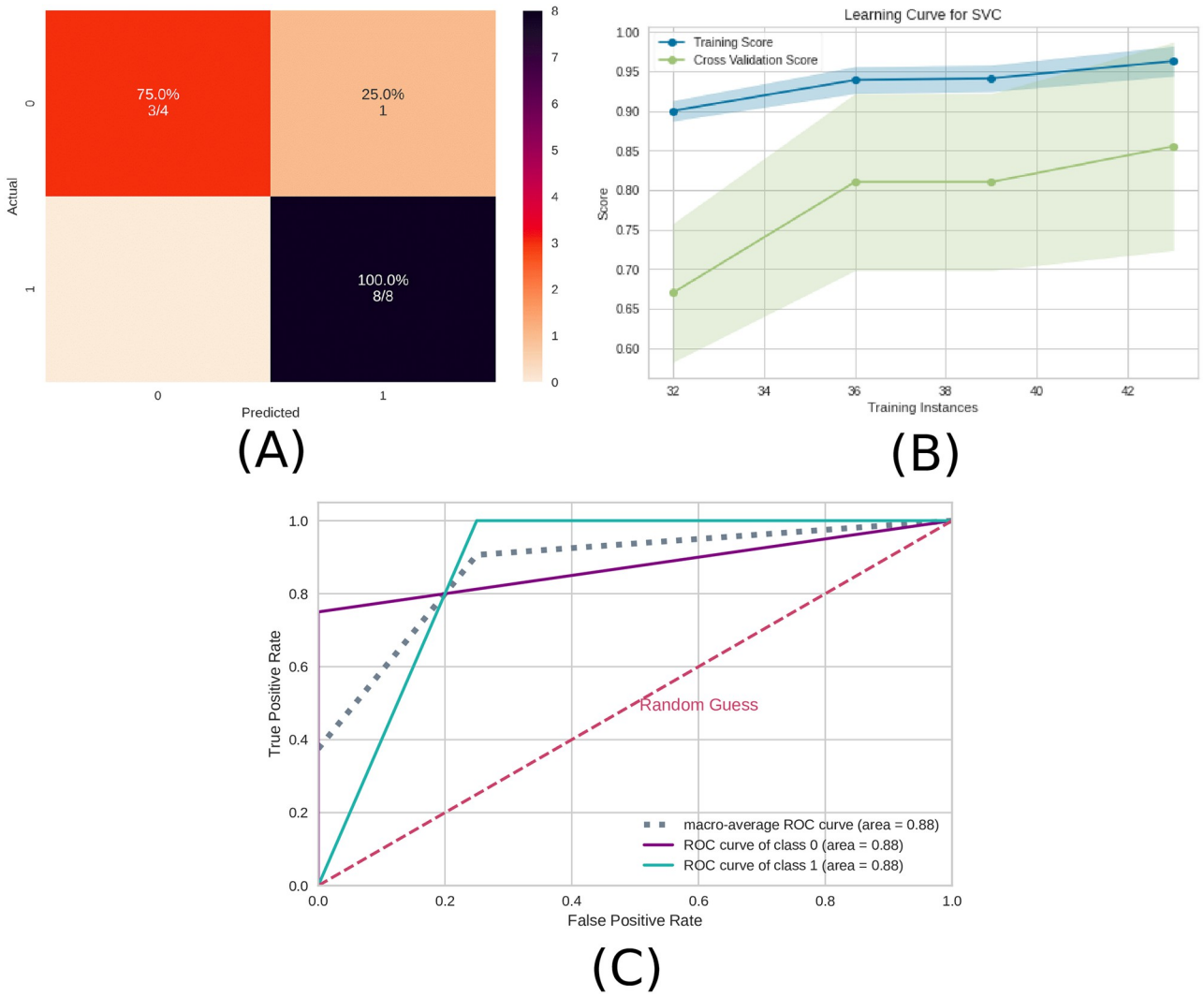

Fig 7. Machine learning results using the connectivity matrices as input data. A) Confusion matrix indicating a true negative rate of 75% (orange according to the color bar) and a true positive of 100% (blue according to the color bar). B) Learning curve for the training accuracy (blue) and for test accuracy (green). C) ROC curve of class 0 (without ayahuasca) and class 1 (with ayahuasca). The gray dotted curve is the macro-average accuracy (area under curve = 0.88) and the pink one the random classifier.

https://doi.org/10.1371/journal.pone.0277257.g007

PO4, low values of correlation (blue dots) were important for detecting the absence of ayahuasca (negative SHAP values), and high values of correlation (red dots) were important for detecting the presence of ayahuasca (positive SHAP values).

The location in the brain can be seen in Fig 9.

3.3 Complex network measures

The test sample performance using the complex network measures was a mean AUC of 0.75, mean accuracy of 0.83, mean F1 score of 0.78, mean recall of 0.75, and mean precision of 0.90.

Similar to the previous subsections 3.1 EEG time series and 3.2 Connectivity matrices, the precision measure was higher than the recall measure, and therefore the model can better detect the presence of ayahuasca.

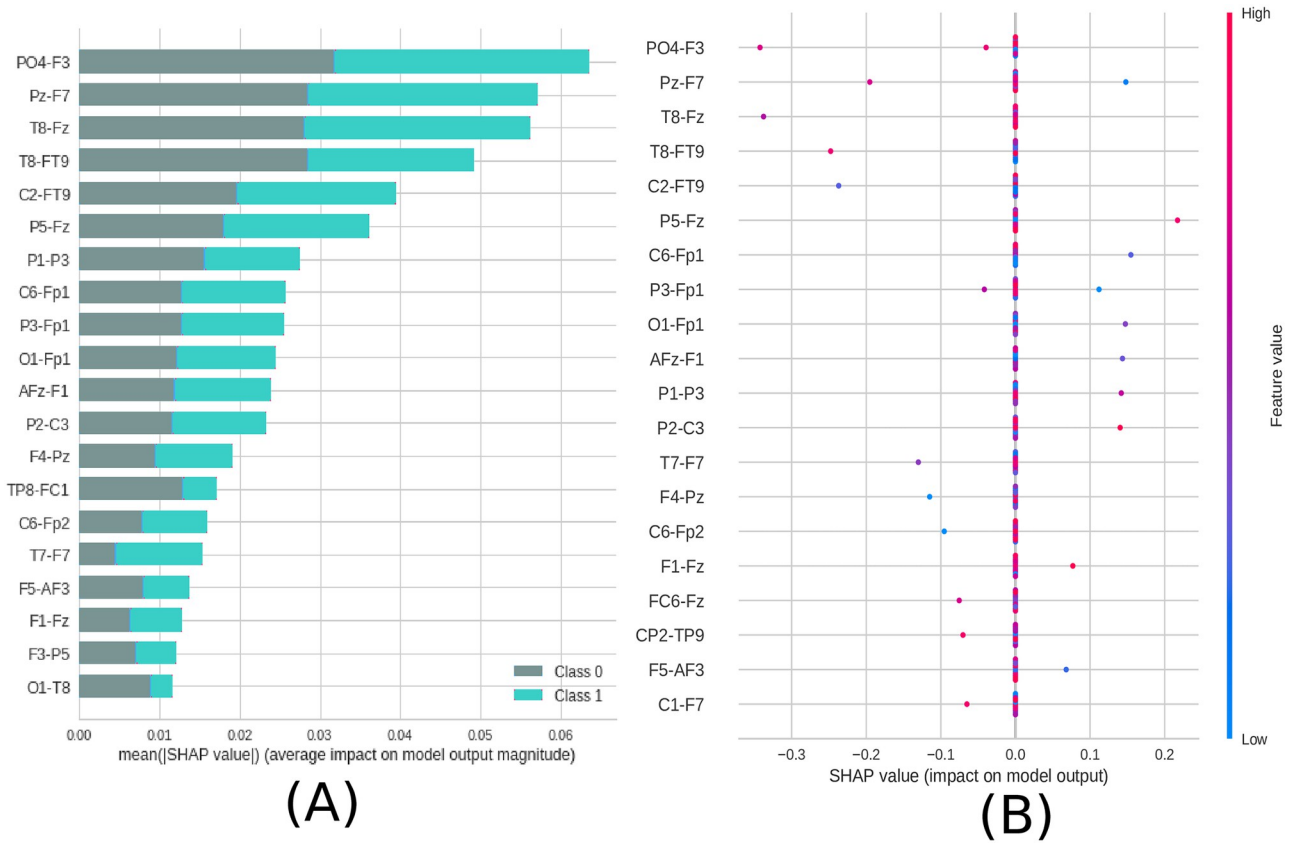

Fig 8. Feature importance ranking for SVM classifier being the connections of brain regions ranked in descending order of importance. The connection between the regions PO4 and F3 is the most important to classify the effect of ayahuasca. A) Feature ranking based on the average of absolute SHAP values over all subjects considering both classes (gray: without ayahuasca, cyan: with ayahuasca). B) Same as A) but additionally showing details of the impact of each feature on the model.

https://doi.org/10.1371/journal.pone.0277257.g008

In Fig 10, the confusion matrix (Fig 10A), the learning curve (Fig 10B), and the ROC curve (Fig 10C) are plotted. Again, the entire database is necessary in order to get the highest accuracy.

From the SHAP values in Fig 11 it can be seen that the most important measure for the model was the CC, followed by assortativity, and the newly introduced measures ASC and ASPC. In addition, in Fig 11B can be seen that for the CC measure, low values of this metric (blue dots) were important for detecting the absence of ayahuasca (negative SHAP values), and high values of this metric (red dots) were important for detecting the presence of ayahuasca (positive SHAP values).

4 Discussion

In this paper, we aimed to answer the question if it is possible to automatically detect brain activity changes due to ayahuasca using machine learning and which features are most important and could act as biomarkers.

Our results show that it is possible to automatically detect the changes due to ayahuasca. The classification accuracy was above 75% for all three data abstraction levels. The classification accuracy of connectivity matrices was higher than the raw EEG time series, suggesting that connection changes are more important between brain regions than within brain regions.

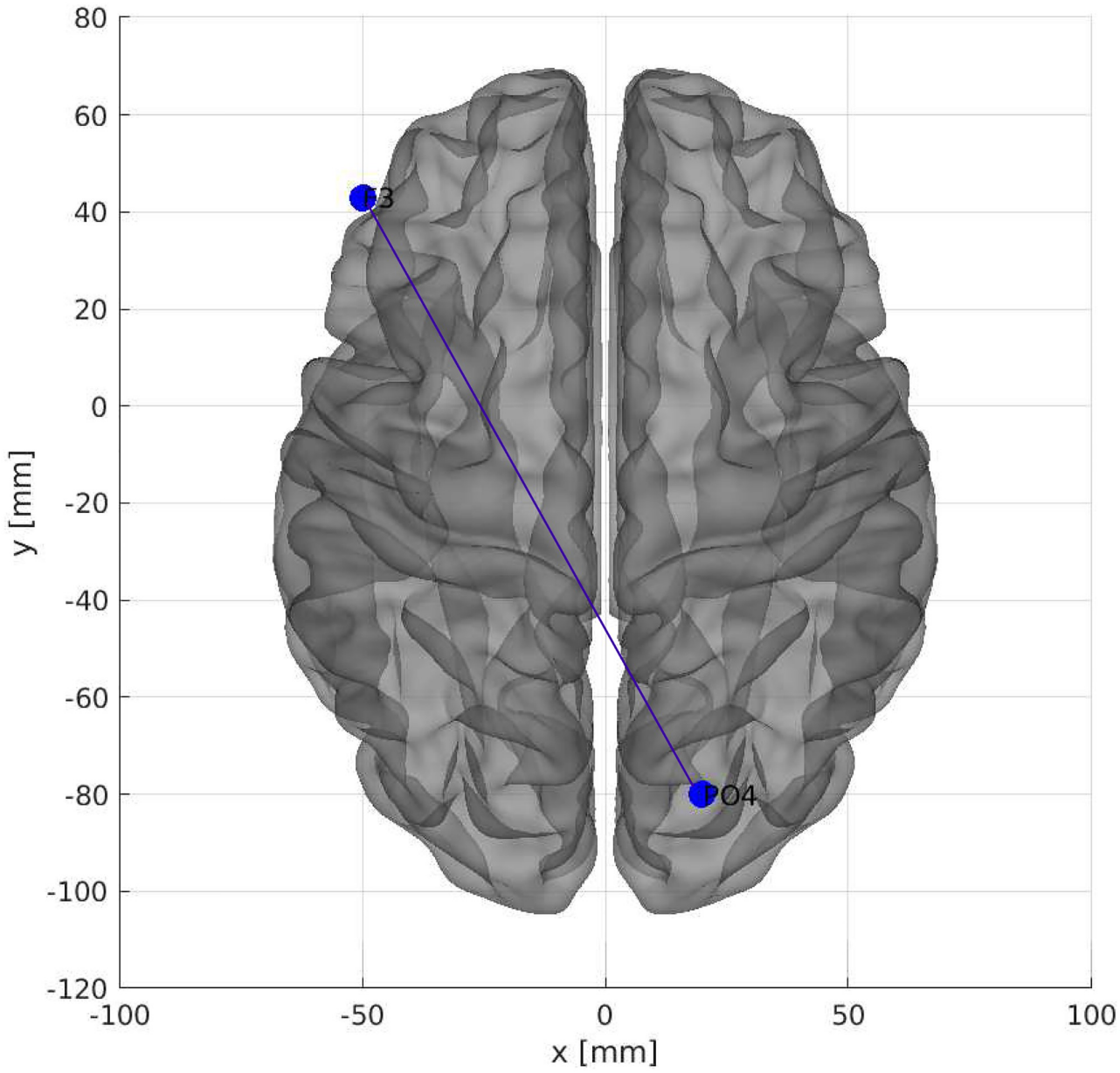

Fig 9. The most important connection of brain regions considering connectivity matrices as input data. Axial dorsal plane showing the brain regions connection between F3 and PO4. The brain plot was made using Braph tool [119], based on the coordinates in [120, 121].

https://doi.org/10.1371/journal.pone.0277257.g009

This result is important since the connectivity matrices improved the accuracy and produced efficiency gains, such as reduced data storage and faster machine learning training. This would be especially useful for larger datasets, where raw time series may be very costly, for example, in hospital diagnosis systems.

4.1 EEG time series

The raw EEG time series analysis revealed that the frontal and the temporal lobe were the most affected brain regions. In line with that, studies using single photon emission computed

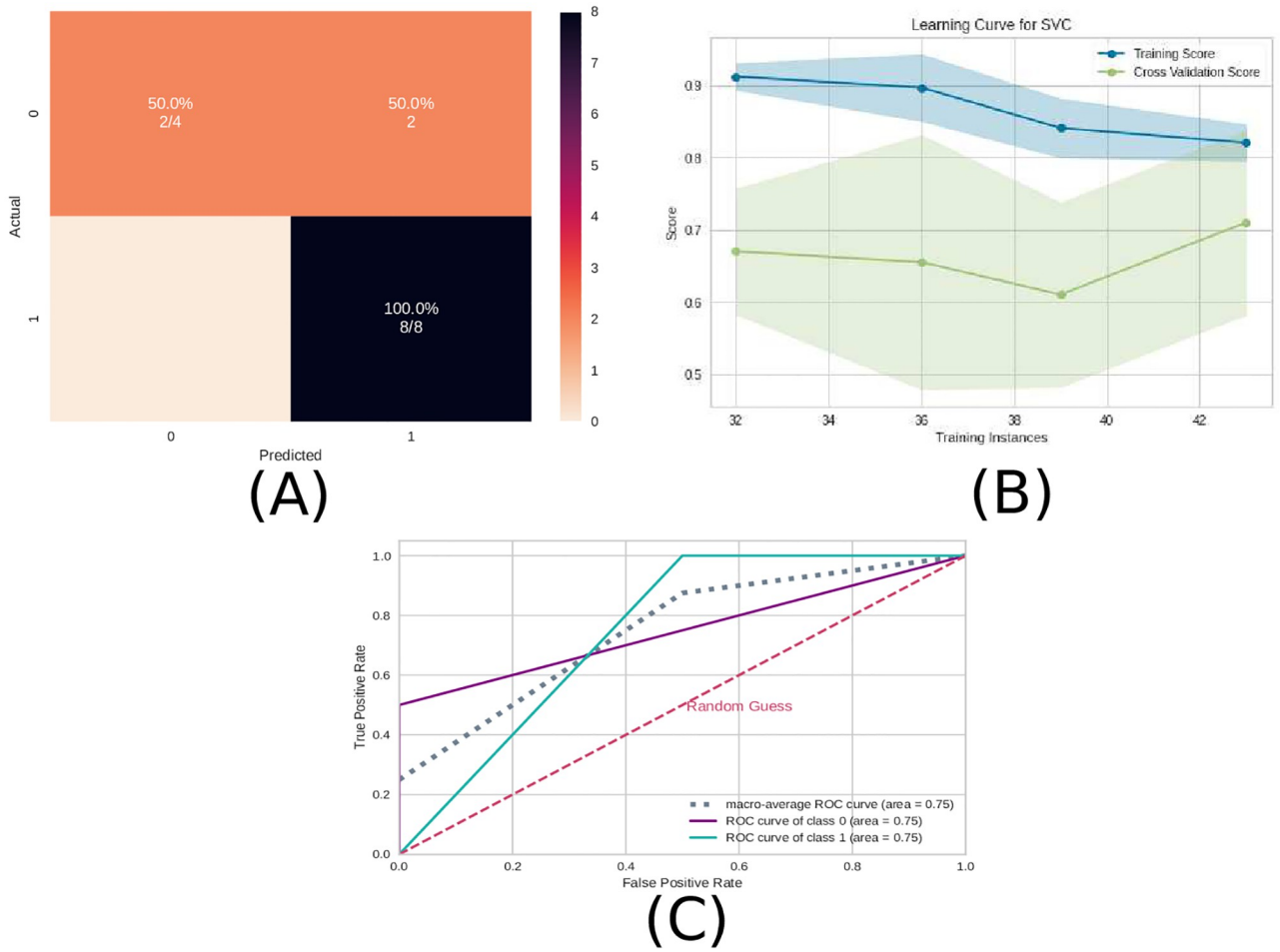

Fig 10. Machine learning results using the complex network measures as input data. A) Confusion matrix indicating a true negative rate of 50% (orange according to the color bar) and a true positive rate of 100% (blue according to the color bar). B) Learning curve for the training accuracy (blue) and for test accuracy (green). C) ROC curve of class 0 (without ayahuasca) and class 1 (with ayahuasca). The gray dotted curve is the macro-average accuracy (area under curve = 0.75) and the pink one the random classifier.

https://doi.org/10.1371/journal.pone.0277257.g010

tomography (SPECT) have reported that ayahuasca increases blood perfusion in the frontal regions of the brain, more specifically, the insula, left nucleus accumbens, left amygdala, parahippocampal gyrus, and left the subgenual area [16, 122]. Furthermore, works using functional magnetic resonance imaging have observed activation in the brain's occipital, temporal, and frontal areas [10, 123]. These regions are related to introspection, emotional processing, and the therapeutic effects of traditional antidepressants [124] and most interestingly, it may also affect motor and cognitive functions in other neurological disorders, such as Parkinson's disease and Alzheimer's disease, respectively [125, 126].

4.2 Connectivity matrices

The correlation between the left frontal cortex (F3) and right parietal-occipital (PO4) was most important in terms of brain connections.

[127] showed that synchronization in the gamma band between the parietal-occipital and frontal cortices was present during face recognition tasks. Since the EEG time series data used

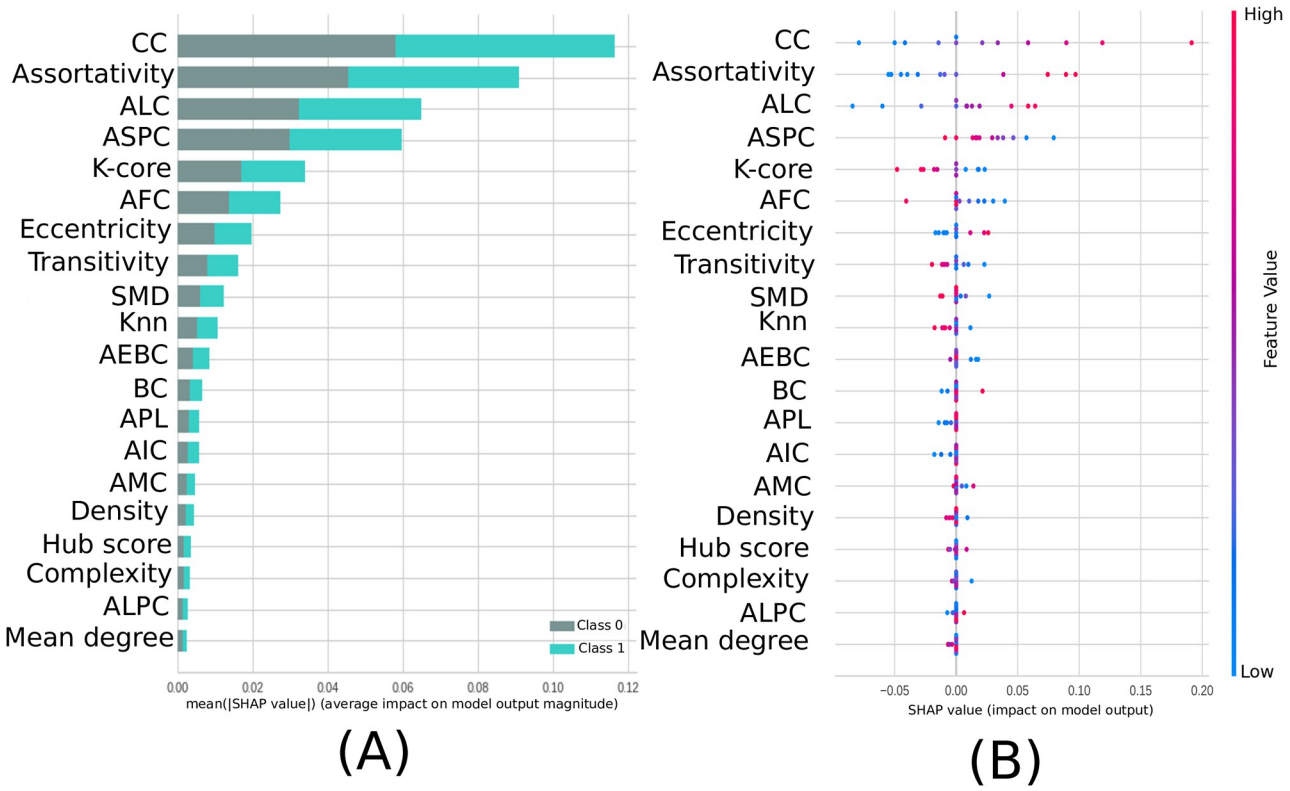

Fig 11. Feature importance ranking for SVM classifier being the features ranked in descending order of importance. The CC measure is the most important to classify the effect of ayahuasca. A) Feature ranking based on the average of absolute SHAP values over all subjects considering both classes (gray: without ayahuasca, cyan: with ayahuasca). B) Same as A) but additionally showing details of the impact of each feature on the model.

https://doi.org/10.1371/journal.pone.0277257.g011

in this work only contained the gamma band, the P04-F3 connection could point to similar cognitive processes in the subjects during ayahuasca-mediated visual hallucinations.

4.3 Complex network measures

The most important complex network measure was CC. CC is a centrality measure that can be defined as the inverse of the average length of the shortest path from one node to all other nodes in the network [128]. The idea is that important nodes participate in many shortest paths within a network and, therefore, play an important role in the flow of information in the brain [93]. The CC was also the most important measure in other papers related to the differentiation of patients with AD [129–132]. In these papers, CC was shown to decrease due to AD disease, while ayahuasca ingestion increased the median value of this measure (see Fig 12).

The second most important complex network measure was assortativity. This measure refers to the resilience of networks [90]. A positive assortativity coefficient indicates a network with a resilient core due to the interconnected nodes of high degree [128]. This measure was also associated with AD in several works [133, 134] whose results showed an increase in the assortativity value in contrast to what was found here, where with the use of ayahuasca, the assortativity value (median) decreased (see on Fig 12). It should be noted that although the median value decreased, the upper confidence interval of the distribution increased.

In summary, the results suggest a possible relationship between ayahuasca and AD in terms of the brain network, indicating a therapeutic potential. Indeed, a possible mechanism of how

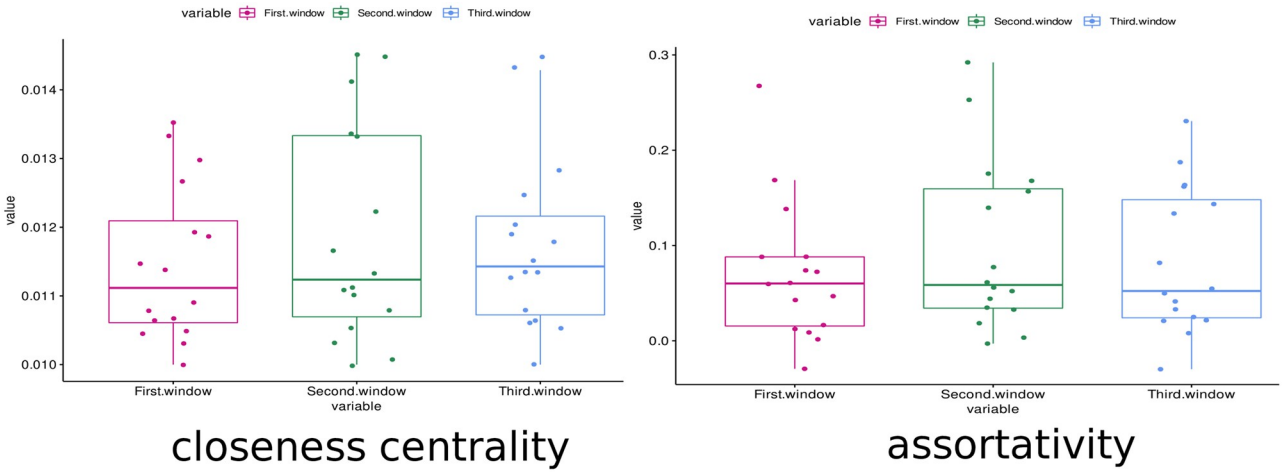

Fig 12. Boxplot of the closeness centrality and assortativity measures. These measures were calculated for all subjects in the first, second and third windows (respectively in pink, green and blue). It can be seen that the median of the closeness centrality measure (central bar in the boxplot) increased with the use of ayahuasca. The median of the assortativity, in contrast, decreased with the use of ayahuasca.

https://doi.org/10.1371/journal.pone.0277257.g012

ayahuasca acts against AD was described in [19]. According to this, the ayahuasca compound dimethyltryptamine (DMT) agonizes the sigma 1 receptor (Sig-1R) and thereby regulates endoplasmic reticulum (ER) stress and Unfolded Protein Response (UPR), which are thought to play a crucial role in neuropsychiatric diseases such as AD.

The seven measures developed here concerning community detection are ranked among the twenty most important measures for classification, with ALC ranking third (see Fig 11). ALC is associated with the size of the largest community found by the leading eigenvector community (LC) detection algorithm. This metric shows increased values (compared to controls) in communities with larger path lengths after the use of ayahuasca (Fig 11B), indicating communities with larger paths after using this psychedelic. Larger brain communities were also found in [135] after the use of ayahuasca. There are two contrasting concepts in the brains of large vertebrates: functional segregation (or specialization) and integration (or distributed processes) [136, 137]. Larger communities also indicate that the balance between functional segregation and integration in the brain was disrupted. This suggests that the distribution of information is slower.

Overall, the classification was successful by considering the complete set of measures rather than just one single measure. As shown in Fig 12, even the most important measures CC and assortativity, did not show much difference between the first window (without ayahuasca) and the other windows (with ayahuasca). Together with the other less important measures, however, the machine learning method was able to distinguish both classes successfully. This leads to the conclusion that a single feature is insufficient as a biomarker, while the different features used in this work may serve as a biomarker.

5 Conclusion

In summary, the results obtained in our study demonstrated that the application of machine learning methods was able to detect changes in brain connectivity during ayahuasca use automatically. Additionally, we demonstrated that the connectivity matrices are the best abstraction level to detect brain changes caused by this psychedelic.

At level abstraction A, our findings suggest that this substance affects important brain regions related to cognitive, psychiatric, and motor functions. These effects may alleviate different symptoms of diseases affecting the brain.

At level abstraction B, the connection between F3 and PO4 is the most important while using ayahuasca according to our classifier model, a significant discovery in psychedelic literature. This connection may point to a cognitive process similar to face recognition in individuals during ayahuasca-mediated visual hallucinations.

Concerning the complex network measures at level abstraction C, CC, assortativity, and one of the new measures developed here, ALC, capture the best brain changes caused by ayahuasca. The new ALC measure inferred that larger communities are associated with this psychedelic and the opposite in its absence. Larger communities suggest that the distribution of information is slower with the use of this substance. Therefore, the present study's findings support that cortical brain activity becomes more entropic under psychoactive substances. [138–140]. There is, however, evidence that psychedelics do not simply make the brain more random, but after the typical organization of the brain is disrupted, strong and topologically far-reaching functional connections emerge which are not present in the natural state of mind.

While our methodology has proven effective, it is focused on the acute evaluation of psychedelics. Consequently, more research is necessary to determine how psychedelics affect the functional connectivity of the brain over the long term using our workflow.

In summary, we have developed a robust computational workflow that provides insights into the mechanism of action of ayahuasca and the interpretability of how it modifies brain networks.

Finally, the same methodology applied here may help interpret EEG time series from patients who consumed other psychedelic drugs, such as pure DMT [141]. In future work, we aim to apply this workflow to recordings from our laboratory using in vitro neuronal networks on microelectrode arrays to study the effects of psychedelics at a single network level. Thus, regardless of the equipment used to collect the data, we would like to verify whether the same method used here can detect changes due to different psychedelics.

Supporting information

S1 Appendix.
(PDF)

Author Contributions

Conceptualization: Caroline L. Alves, Francisco A. Rodrigues, Manuel Ciba.

Data curation: Caroline L. Alves, Francisco A. Rodrigues, Manuel Ciba.

Formal analysis: Caroline L. Alves, Rubens Gisbert Cury, Kirstin Roster, Aruane M. Pineda, Francisco A. Rodrigues, Manuel Ciba.

Funding acquisition: Francisco A. Rodrigues, Christiane Thielemann.

Investigation: Caroline L. Alves, Rubens Gisbert Cury, Kirstin Roster, Aruane M. Pineda, Francisco A. Rodrigues, Christiane Thielemann, Manuel Ciba.

Methodology: Caroline L. Alves.

Project administration: Christiane Thielemann, Manuel Ciba.

Resources: Francisco A. Rodrigues, Christiane Thielemann.

Supervision: Francisco A. Rodrigues, Christiane Thielemann, Manuel Ciba.

Validation: Caroline L. Alves, Rubens Gisbert Cury, Kirstin Roster, Aruane M. Pineda, Francisco A. Rodrigues, Manuel Ciba.

Visualization: Caroline L. Alves.

Writing – original draft: Caroline L. Alves, Rubens Gisbert Cury, Kirstin Roster, Francisco A. Rodrigues, Christiane Thielemann, Manuel Ciba.

Writing – review & editing: Caroline L. Alves, Aruane M. Pineda.

References

1. Metzner R. Hallucinogenic drugs and plants in psychotherapy and shamanism. Journal of psychoactive drugs. 1998; 30(4):333–341. https://doi.org/10.1080/02791072.1998.10399709 PMID: 9924839
2. de Araújo DB. Evidence for the therapeutic effects of Ayahuasca. Advances in psychedelic medicine State-of-the-art therapeutic applications. 2019; p. 103–23.
3. Bouso JC, Riba J. Ayahuasca and the treatment of drug addiction. In: The therapeutic use of ayahuasca. Springer; 2014. p. 95–109.
4. Fernández X, Fábregas JM. Experience of treatment with ayahuasca for drug addiction in the Brazilian Amazon. In: The therapeutic use of ayahuasca. Springer; 2014. p. 161–182.
5. Giovannetti C, Garcia Arce S, Rush B, Mendive F. Pilot evaluation of a residential drug addiction treatment combining traditional Amazonian medicine, ayahuasca and psychotherapy on depression and anxiety. Journal of Psychoactive Drugs. 2020; 52(5):472–481. https://doi.org/10.1080/02791072.2020.1789247 PMID: 32748709
6. Serrano-Dueñas M, Cardozo-Pelaez F, Sánchez-Ramos JR. Effects of Banisteriopsis caapi extract on Parkinson's disease. The Scientific Review of Alternative Medicine. 2001; 5(3):127–132.
7. Wang YH, Samoylenko V, Tekwani BL, Khan IA, Miller LS, Chaurasiya ND, et al. Composition, standardization and chemical profiling of Banisteriopsis caapi, a plant for the treatment of neurodegenerative disorders relevant to Parkinson's disease. Journal of ethnopharmacology. 2010; 128(3):662–671. https://doi.org/10.1016/j.jep.2010.02.013 PMID: 20219660
8. Katchborian-Neto A, Santos WT, Nicácio KJ, Corrêa JO, Murgu M, Martins TM, et al. Neuroprotective potential of Ayahuasca and untargeted metabolomics analyses: applicability to Parkinson's disease. Journal of ethnopharmacology. 2020; 255:112743. https://doi.org/10.1016/j.jep.2020.112743 PMID: 32171895
9. Brierley DI, Davidson C. Developments in harmine pharmacology—Implications for ayahuasca use and drug-dependence treatment. Progress in neuro-psychopharmacology and biological psychiatry. 2012; 39(2):263–272. https://doi.org/10.1016/j.pnpbp.2012.06.001 PMID: 22691716
10. Jiménez-Garrido DF, Gémez-Sousa M, Ona G, Dos Santos RG, Hallak JE, Alcázar-Cércoles Mé, et al. Effects of ayahuasca on mental health and quality of life in naïve users: A longitudinal and cross-sectional study combination. Scientific reports. 2020; 10(1):1–12. https://doi.org/10.1038/s41598-020-61169-x PMID: 32139811
11. Palhano-Fontes F, Barreto D, Onias H, Andrade KC, Novaes MM, Pessoa JA, et al. Rapid antidepressant effects of the psychedelic ayahuasca in treatment-resistant depression: a randomized placebo-controlled trial. Psychological medicine. 2019; 49(4):655–663. https://doi.org/10.1017/S0033291718001356 PMID: 29903051
12. Sanches RF, de Lima Osério F, Dos Santos RG, Macedo LR, Maia-de Oliveira JP, Wichert-Ana L, et al. Antidepressant effects of a single dose of ayahuasca in patients with recurrent depression: a SPECT study. Journal of clinical psychopharmacology. 2016; 36(1):77–81. https://doi.org/10.1097/JCP.0000000000000436 PMID: 26650973
13. Palhano-Fontes F, Mota-Rolim S, Lobão-Soares B, Galvão-Coelho N, Maia-Oliveira JP, Araújo DB. Recent Evidence on the Antidepressant Effects of Ayahuasca. Ayahuasca Healing and Science. 2021; p. 21. https://doi.org/10.1007/978-3-030-55688-4_2
14. de Lima Osério F, de Macedo LRH, de Sousa JPM, Pinto JP, Quevedo J, de Souza Crippa JA, et al. The therapeutic potential of harmine and ayahuasca in depression: Evidence from exploratory animal and human studies. The ethnopharmacology of ayahuasca. 2011; 75:85.
15. Frood A. Ayahuasca psychedelic tested for depression. Nature News. 2015;. https://doi.org/10.1038/nature.2015.17252

16. Dos Santos RG, Osério FL, Crippa JAS, Riba J, Zuardi AW, Hallak JE. Antidepressive, anxiolytic, and antiaddictive effects of ayahuasca, psilocybin and lysergic acid diethylamide (LSD): a systematic review of clinical trials published in the last 25 years. Therapeutic advances in psychopharmacology. 2016; 6(3):193–213. https://doi.org/10.1177/2045125316638008 PMID: 27354908

17. Morales-García JA, de la Fuente Revenga M, Alonso-Gil S, Rodríguez-Franco MI, Feilding A, Perez-Castillo A, et al. The alkaloids of Banisteriopsis caapi, the plant source of the Amazonian hallucinogen Ayahuasca, stimulate adult neurogenesis in vitro. Scientific reports. 2017; 7(1):1–13. https://doi.org/10.1038/s41598-017-05407-9 PMID: 28706205

18. da Silva MG, Daros GC, de Bitencourt RM. Anti-inflammatory activity of ayahuasca and its implications for the treatment of neurological and psychiatric diseases. Behavioural Brain Research. 2020; p. 113003. PMID: 33166569

19. Frecska E, Bokor P, Winkelman M. The therapeutic potentials of ayahuasca: possible effects against various diseases of civilization. Frontiers in pharmacology. 2016; 7:35. https://doi.org/10.3389/fphar.2016.00035 PMID: 26973523

20. Dos Santos RG, Hallak JE. Effects of the natural β-carboline alkaloid harmine, a main constituent of ayahuasca, in memory and in the hippocampus: A systematic literature review of preclinical studies. Journal of psychoactive drugs. 2017; 49(1):1–10. https://doi.org/10.1080/02791072.2016.1260189 PMID: 27918874

21. Schenberg EE, Alexandre JFM, Filev R, Cravo AM, Sato JR, Muthukumaraswamy SD, et al. Acute biphasic effects of ayahuasca. PloS one. 2015; 10(9):e0137202. https://doi.org/10.1371/journal.pone.0137202 PMID: 26421727

22. Bassett DS, Gazzaniga MS. Understanding complexity in the human brain. Trends in cognitive sciences. 2011; 15(5):200–209. https://doi.org/10.1016/j.tics.2011.03.006 PMID: 21497128

23. Pineda AM, Ramos FM, Betting LE, Campanharo AS. Quantile graphs for EEG-based diagnosis of Alzheimer's disease. Plos one. 2020; 15(6):e0231169. https://doi.org/10.1371/journal.pone.0231169 PMID: 32502204

24. Sporns O. Graph theory methods: applications in brain networks. Dialogues in clinical neuroscience. 2018; 20(2):111. https://doi.org/10.31887/DCNS.2018.20.2/osporns PMID: 30250388

25. Bassett DS, Zurn P, Gold JI. On the nature and use of models in network neuroscience. Nature Reviews Neuroscience. 2018; 19(9):566–578. https://doi.org/10.1038/s41583-018-0038-8 PMID: 30002509

26. Hayashida M, Akutsu T. Complex network-based approaches to biomarker discovery. Biomarkers in medicine. 2016; 10(6):621–632. https://doi.org/10.2217/bmm-2015-0047 PMID: 26947205

27. Fekete T, Zach N, Mujica-Parodi LR, Turner MR. Multiple kernel learning captures a systems-level functional connectivity biomarker signature in amyotrophic lateral sclerosis. PloS one. 2013; 8(12):e85190. https://doi.org/10.1371/journal.pone.0085190 PMID: 24391997

28. Newman ME. Communities, modules and large-scale structure in networks. Nature physics. 2012; 8(1):25–31. https://doi.org/10.1038/nphys2162

29. Kim J, Lee JG. Community detection in multi-layer graphs: A survey. ACM SIGMOD Record. 2015; 44(3):37–48. https://doi.org/10.1145/2854006.2854013

30. Zhao X, Liang J, Wang J. A community detection algorithm based on graph compression for large-scale social networks. Information Sciences. 2021; 551:358–372. https://doi.org/10.1016/j.ins.2020.10.057

31. Lung RI, Suciu M, Meszlényi R, Buza K, Gaské N. Community structure detection for the functional connectivity networks of the brain. In: International Conference on Parallel Problem Solving from Nature. Springer; 2016. p. 633–643.

32. Khajehpour H, Makkiabadi B, Ekhtiari H, Bakht S, Noroozi A, Mohagheghian F. Disrupted resting-state brain functional network in methamphetamine abusers: A brain source space study by EEG. PloS one. 2019; 14(12):e0226249.

33. Varley TF, Craig M, Adapa R, Finoia P, Williams G, Allanson J, et al. Fractal dimension of cortical functional connectivity networks & severity of disorders of consciousness. PLoS One. 2020; 15(2):e0223812. https://doi.org/10.1371/journal.pone.0223812 PMID: 32053587

34. Song CW, Jung H, Chung K. Development of a medical big-data mining process using topic modeling. Cluster Computing. 2019; 22(1):1949–1958. https://doi.org/10.1007/s10586-017-0942-0

35. Mozaffarinya M, Shahriyari AR, Bahadori MK, Ghazvini A, Athari SS, Vahedi G. A data-mining algorithm to assess key factors in asthma diagnosis. Revue Française d'Allergologie. 2019;.

36. Ilyasova N, Kupriyanov A, Paringer R, Kirsh D. Particular use of BIG DATA in medical diagnostic tasks. Pattern Recognition and Image Analysis. 2018; 28(1):114–121. https://doi.org/10.1134/S1054661818010066

37. Li RC, Asch SM, Shah NH. Developing a delivery science for artificial intelligence in healthcare. NPJ digital medicine. 2020; 3(1):1–3. https://doi.org/10.1038/s41746-020-00318-y PMID: 32885053

38. Bellazzi R, Zupan B. Predictive data mining in clinical medicine: current issues and guidelines. International journal of medical informatics. 2008; 77(2):81–97. https://doi.org/10.1016/j.ijmedinf.2006.11.006 PMID: 17188928

39. Buza K. Asterics: Projection-based classification of eeg with asymmetric loss linear regression and genetic algorithm. In: 2020 IEEE 14th International Symposium on Applied Computational Intelligence and Informatics (SACI). IEEE; 2020. p. 000035–000040.

40. Abel JH, Badgeley MA, Meschede-Krasa B, Schamberg G, Garwood IC, Lecamwasam K, et al. Machine learning of EEG spectra classifies unconsciousness during GABAergic anesthesia. Plos one. 2021; 16(5):e0246165. https://doi.org/10.1371/journal.pone.0246165 PMID: 33956800

41. Alves CL, Pineda AM, Roster K, Thielemann C, Rodrigues FA. EEG functional connectivity and deep learning for automatic diagnosis of brain disorders: Alzheimer's disease and schizophrenia. Journal of Physics: Complexity. 2022; 3(2):025001.

42. Jayarathne I, Cohen M, Amarakeerthi S. Person identification from EEG using various machine learning techniques with inter-hemispheric amplitude ratio. PloS one. 2020; 15(9):e0238872. https://doi.org/10.1371/journal.pone.0238872 PMID: 32915850

43. Bowen D, Ungar L. Generalized SHAP: Generating multiple types of explanations in machine learning. arXiv preprint arXiv:200607155. 2020;.

44. Rodríguez-Pérez R, Bajorath J. Interpretation of compound activity predictions from complex machine learning models using local approximations and shapley values. Journal of Medicinal Chemistry. 2019; 63(16):8761–8777. PMID: 31512867

45. Spadon G, de Carvalho AC, Rodrigues-Jr JF, Alves LG. Reconstructing commuters network using machine learning and urban indicators. Scientific reports. 2019; 9(1):1–13. https://doi.org/10.1038/s41598-019-48295-x PMID: 31409862

46. Johnson MW, Richards WA, Griffiths RR. Human hallucinogen research: guidelines for safety. Journal of psychopharmacology. 2008; 22(6):603–620. https://doi.org/10.1177/0269881108093587 PMID: 18593734

47. Bottou L, Lin CJ. Support vector machine solvers. Large scale kernel machines. 2007; 3(1):301–320.

48. Mazrooyisebdani M, Nair VA, Garcia-Ramos C, Mohanty R, Meyerand E, Hermann B, et al. Graph theory analysis of functional connectivity combined with machine learning approaches demonstrates widespread network differences and predicts clinical variables in temporal lobe epilepsy. Brain connectivity. 2020; 10(1):39–50. https://doi.org/10.1089/brain.2019.0702 PMID: 31984759

49. Diykh M, Li Y, Wen P. Classify epileptic EEG signals using weighted complex networks based community structure detection. Expert Systems with Applications. 2017; 90:87–100. https://doi.org/10.1016/j.eswa.2017.08.012

50. Dey S, Rao AR, Shah M. Attributed graph distance measure for automatic detection of attention deficit hyperactive disordered subjects. Frontiers in neural circuits. 2014; 8:64. https://doi.org/10.3389/fncir.2014.00064 PMID: 24982615

51. Breiman L. Random forests. Machine learning. 2001; 45(1):5–32. https://doi.org/10.1023/A:1010933404324

52. Friedman N, Geiger D, Goldszmidt M. Bayesian network classifiers. Machine learning. 1997; 29 (2):131–163. https://doi.org/10.1023/A:1007465528199

53. Hinton G, Rumelhart D, Williams R. Learning internal representations by error propagation. Parallel distributed processing. 1986; 1:318–362.

54. Zhang T. Solving large scale linear prediction problems using stochastic gradient descent algorithms. In: Proceedings of the twenty-first international conference on Machine learning; 2004. p. 116.

55. Tolles J, Meurer WJ. Logistic regression: relating patient characteristics to outcomes. Jama. 2016; 316(5):533–534. https://doi.org/10.1001/jama.2016.7653 PMID: 27483067

56. Friedman JH. Greedy function approximation: a gradient boosting machine. Annals of statistics. 2001; p. 1189–1232.

57. Refaeilzadeh P, Tang L, Liu H. Cross-validation. Encyclopedia of database systems. 2009; 5:532–538. https://doi.org/10.1007/978-0-387-39940-9_565

58. Berrar D. Cross-Validation.; 2019.

59. Bengio Y, Grandvalet Y. No unbiased estimator of the variance of k-fold cross-validation. Journal of machine learning research. 2004; 5(Sep):1089–1105.

60. Shah AA, Khan YD. Identification of 4-carboxyglutamate residue sites based on position based statistical feature and multiple classification. Scientific Reports. 2020; 10(1):1–10. https://doi.org/10.1038/s41598-020-73107-y PMID: 33037248

61. Kawamoto T, Kabashima Y. Cross-validation estimate of the number of clusters in a network. Scientific reports. 2017; 7(1):1–17. https://doi.org/10.1038/s41598-017-03623-x PMID: 28607441

62. Chan J, Rea T, Gollakota S, Sunshine JE. Contactless cardiac arrest detection using smart devices. NPJ digital medicine. 2019; 2(1):1–8. https://doi.org/10.1038/s41746-019-0128-7 PMID: 31304398

63. Sato M, Morimoto K, Kajihara S, Tateishi R, Shiina S, Koike K, et al. Machine-learning approach for the development of a novel predictive model for the diagnosis of hepatocellular carcinoma. Scientific reports. 2019; 9(1):1–7. https://doi.org/10.1038/s41598-019-44022-8 PMID: 31147560

64. Zhong Z, Yuan X, Liu S, Yang Y, Liu F. Machine learning prediction models for prognosis of critically ill patients after open-heart surgery. Scientific Reports. 2021; 11(1):1–10. https://doi.org/10.1038/s41598-021-83020-7 PMID: 33564090

65. Arcadu F, Benmansour F, Maunz A, Willis J, Haskova Z, Prunotto M. Author Correction: Deep learning algorithm predicts diabetic retinopathy progression in individual patients. NPJ digital medicine. 2020; 3(1):1–6. https://doi.org/10.1038/s41746-020-00365-5 PMID: 33293570

66. Krittanawong C, Virk HUH, Kumar A, Aydar M, Wang Z, Stewart MP, et al. Machine learning and deep learning to predict mortality in patients with spontaneous coronary artery dissection. Scientific reports. 2021; 11(1):1–10. https://doi.org/10.1038/s41598-021-88172-0 PMID: 33903608

67. Rashidi HH, Sen S, Palmieri TL, Blackmon T, Wajda J, Tran NK. Early recognition of burn-and trauma-related acute kidney injury: a pilot comparison of machine learning techniques. Scientific reports. 2020; 10(1):1–9. https://doi.org/10.1038/s41598-019-57083-6 PMID: 31937795

68. Mincholé A, Rodriguez B. Artificial intelligence for the electrocardiogram. Nature medicine. 2019; 25(1):22–23. https://doi.org/10.1038/s41591-018-0306-1 PMID: 30617324

69. Tolkach Y, Dohmgörgen T, Toma M, Kristiansen G. High-accuracy prostate cancer pathology using deep learning. Nature Machine Intelligence. 2020; 2(7):411–418. https://doi.org/10.1038/s42256-020-0200-7

70. Dukart J, Weis S, Genon S, Eickhoff SB. Towards increasing the clinical applicability of machine learning biomarkers in psychiatry. Nature Human Behaviour. 2021; 5(4):431–432. https://doi.org/10.1038/s41562-021-01085-w PMID: 33820977

71. Park Y, Kellis M. Deep learning for regulatory genomics. Nature biotechnology. 2015; 33(8):825–826. https://doi.org/10.1038/nbt.3313 PMID: 26252139

72. Ito Y, Unagami M, Yamabe F, Mitsui Y, Nakajima K, Nagao K, et al. A method for utilizing automated machine learning for histopathological classification of testis based on Johnsen scores. Scientific reports. 2021; 11(1):1–11. https://doi.org/10.1038/s41598-021-89369-z PMID: 33967273

73. Kim J, Lee J, Park E, Han J. A deep learning model for detecting mental illness from user content on social media. Scientific reports. 2020; 10(1):1–6. https://doi.org/10.1038/s41598-020-68764-y PMID: 32678250

74. Li Y, Nowak CM, Pham U, Nguyen K, Bleris L. Cell morphology-based machine learning models for human cell state classification. NPJ systems biology and applications. 2021; 7(1):1–9. https://doi.org/10.1038/s41540-021-00180-y PMID: 34039992

75. Yu X, Pang W, Xu Q, Liang M. Mammographic image classification with deep fusion learning. Scientific Reports. 2020; 10(1):1–11. https://doi.org/10.1038/s41598-020-71431-x PMID: 32873872

76. Berryman S, Matthews K, Lee JH, Duffy SP, Ma H. Image-based phenotyping of disaggregated cells using deep learning. Communications Biology. 2020; 3(1):1–9. https://doi.org/10.1038/s42003-020-01399-x PMID: 33188302

77. Yang S, Kweon J, Roh JH, Lee JH, Kang H, Park LJ, et al. Deep learning segmentation of major vessels in X-ray coronary angiography. Scientific reports. 2019; 9(1):1–11. https://doi.org/10.1038/s41598-019-53254-7 PMID: 31729445

78. Hannun AY, Rajpurkar P, Haghpanahi M, Tison GH, Bourn C, Turakhia MP, et al. Cardiologist-level arrhythmia detection and classification in ambulatory electrocardiograms using a deep neural network. Nature medicine. 2019; 25(1):65–69. https://doi.org/10.1038/s41591-018-0268-3 PMID: 30617320

79. Bracher-Smith M, Crawford K, Escott-Price V. Machine learning for genetic prediction of psychiatric disorders: a systematic review. Molecular Psychiatry. 2021; 26(1):70–79. https://doi.org/10.1038/s41380-020-0825-2 PMID: 32591634

80. Patel D, Kher V, Desai B, Lei X, Cen S, Nanda N, et al. Machine learning based predictors for COVID-19 disease severity. Scientific Reports. 2021; 11(1):1–7. https://doi.org/10.1038/s41598-021-83967-7 PMID: 33633145

81. Lundberg SM, Lee SI. A unified approach to interpreting model predictions. In: Proceedings of the 31st international conference on neural information processing systems; 2017. p. 4768–4777.

82. Cerqueira V, Torgo L, Mozetič I. Evaluating time series forecasting models: An empirical study on performance estimation methods. Machine Learning. 2020; 109(11):1997–2028. https://doi.org/10.1007/s10994-020-05910-7

83. Bouktif S, Fiaz A, Ouni A, Serhani MA. Optimal deep learning lstm model for electric load forecasting using feature selection and genetic algorithm: Comparison with machine learning approaches. Energies. 2018; 11(7):1636. https://doi.org/10.3390/en11071636

84. Rojas GM, Alvarez C, Montoya CE, de la Iglesia-Vayá M, Cisternas JE, Gálvez M. Study of resting-state functional connectivity networks using EEG electrodes position as seed. Frontiers in neuroscience. 2018; 12:235. https://doi.org/10.3389/fnins.2018.00235 PMID: 29740268

85. Wang L, Wang W, Yan T, Song J, Yang W, Wang B, et al. Beta-band functional connectivity influences audiovisual integration in older age: an EEG study. Frontiers in aging neuroscience. 2017; 9:239. https://doi.org/10.3389/fnagi.2017.00239 PMID: 28824411

86. Jalili M. Functional brain networks: does the choice of dependency estimator and binarization method matter? Scientific reports. 2016; 6(1):1–12. https://doi.org/10.1038/srep29780 PMID: 27417262

87. Han C, Sun X, Yang Y, Che Y, Qin Y. Brain complex network characteristic analysis of fatigue during simulated driving based on electroencephalogram signals. Entropy. 2019; 21(4):353. https://doi.org/10.3390/e21040353 PMID: 33267067

88. Tokariev A, Roberts JA, Zalesky A, Zhao X, Vanhatalo S, Breakspear M, et al. Large-scale brain modes reorganize between infant sleep states and carry prognostic information for preterms. Nature communications. 2019; 10(1):1–9. https://doi.org/10.1038/s41467-019-10467-8 PMID: 31197175

89. Newman ME. The structure and function of complex networks. SIAM review. 2003; 45(2):167–256. https://doi.org/10.1137/S003614450342480

90. Newman ME. Assortative mixing in networks. Physical review letters. 2002; 89(20):208701. https://doi.org/10.1103/PhysRevLett.89.208701 PMID: 12443515

91. Albert R, Barabási AL. Statistical mechanics of complex networks. Reviews of modern physics. 2002; 74(1):47. https://doi.org/10.1103/RevModPhys.74.47

92. Freeman LC. A set of measures of centrality based on betweenness. Sociometry. 1977; p. 35–41. https://doi.org/10.2307/3033543

93. Freeman LC. Centrality in social networks conceptual clarification. Social networks. 1978; 1(3):215–239. https://doi.org/10.1016/0378-8733(78)90021-7

94. Bonacich P. Power and centrality: A family of measures. American journal of sociology. 1987; 92 (5):1170–1182. https://doi.org/10.1086/228631

95. Albert R, Jeong H, Barabási AL. Diameter of the world-wide web. nature. 1999; 401(6749):130–131. https://doi.org/10.1038/43601

96. Kleinberg JM. Hubs, authorities, and communities. ACM computing surveys (CSUR). 1999; 31 (4es):5–es.

97. Eppstein D, Paterson MS, Yao FF. On nearest-neighbor graphs. Discrete & Computational Geometry. 1997; 17(3):263–282. https://doi.org/10.1007/PL00009293

98. Doyle J, Graver J. Mean distance in a graph. Discrete Mathematics. 1977; 17(2):147–154. https://doi.org/10.1016/0012-365X(77)90144-3

99. Snijders TA. The degree variance: an index of graph heterogeneity. Social networks. 1981; 3(3):163–174. https://doi.org/10.1016/0378-8733(81)90014-9

100. Dehmer M, Mowshowitz A. A history of graph entropy measures. Information Sciences. 2011; 181 (1):57–78. https://doi.org/10.1016/j.ins.2010.08.041

101. Watts DJ, Strogatz SH. Collective dynamics of 'small-world'networks. Nature. 1998; 393(6684):440–442. https://doi.org/10.1038/30918 PMID: 9623998

102. Newman ME, Watts DJ, Strogatz SH. Random graph models of social networks. Proceedings of the National Academy of Sciences. 2002; 99(suppl 1):2566–2572. https://doi.org/10.1073/pnas.012582999 PMID: 11875211

103. Seidman SB. Network structure and minimum degree. Social networks. 1983; 5(3):269–287. https://doi.org/10.1016/0378-8733(83)90028-X

104. Newman M. Networks: an introduction. Oxford university press; 2010.

105. Hage P, Harary F. Eccentricity and centrality in networks. Social networks. 1995; 17(1):57–63. https://doi.org/10.1016/0378-8733(94)00248-9

106. Anderson BS, Butts C, Carley K. The interaction of size and density with graph-level indices. Social networks. 1999; 21(3):239–267. https://doi.org/10.1016/S0378-8733(99)00011-8

107. Latora V, Marchiori M. Economic small-world behavior in weighted networks. The European Physical Journal B-Condensed Matter and Complex Systems. 2003; 32(2):249–263. https://doi.org/10.1140/epjb/e2003-00095-5

108. Clauset A, Newman ME, Moore C. Finding community structure in very large networks. Physical review E. 2004; 70(6):066111. https://doi.org/10.1103/PhysRevE.70.066111 PMID: 15697438

109. Girvan M, Newman ME. Community structure in social and biological networks. Proceedings of the national academy of sciences. 2002; 99(12):7821–7826. https://doi.org/10.1073/pnas.122653799 PMID: 12060727

110. Rosvall M, Axelsson D, Bergstrom CT. The map equation. The European Physical Journal Special Topics. 2009; 178(1):13–23. https://doi.org/10.1140/epjst/e2010-01179-1

111. Huffman DA. A method for the construction of minimum-redundancy codes. Proceedings of the IRE. 1952; 40(9):1098–1101. https://doi.org/10.1109/JRPROC.1952.273898

112. Newman ME. Finding community structure in networks using the eigenvectors of matrices. Physical review E. 2006; 74(3):036104. https://doi.org/10.1103/PhysRevE.74.036104 PMID: 17025705

113. Raghavan UN, Albert R, Kumara S. Near linear time algorithm to detect community structures in large-scale networks. Physical review E. 2007; 76(3):036106. https://doi.org/10.1103/PhysRevE.76.036106 PMID: 17930305

114. Barber MJ, Clark JW. Detecting network communities by propagating labels under constraints. Physical Review E. 2009; 80(2):026129. https://doi.org/10.1103/PhysRevE.80.026129 PMID: 19792222

115. Li H, Zhang R, Zhao Z, Liu X. LPA-MNI: an improved label propagation algorithm based on modularity and node importance for community detection. Entropy. 2021; 23(5):497. https://doi.org/10.3390/e23050497 PMID: 33919470

116. Reichardt J, Bornholdt S. Statistical mechanics of community detection. Physical review E. 2006; 74 (1):016110. https://doi.org/10.1103/PhysRevE.74.016110 PMID: 16907154

117. Chejara P, Godfrey WW. Comparative analysis of community detection algorithms. In: 2017 Conference on Information and Communication Technology (CICT). IEEE; 2017. p. 1–5.

118. Blondel VD, Guillaume JL, Lambiotte R, Lefebvre E. Fast unfolding of communities in large networks. Journal of statistical mechanics: theory and experiment. 2008; 2008(10):P10008. https://doi.org/10.1088/1742-5468/2008/10/P10008

119. Mijalkov M, Kakaei E, Pereira JB, Westman E, Volpe G, Initiative ADN. BRAPH: a graph theory software for the analysis of brain connectivity. PloS one. 2017; 12(8):e0178798. https://doi.org/10.1371/journal.pone.0178798 PMID: 28763447

120. Michel CM, Brunet D. EEG source imaging: a practical review of the analysis steps. Frontiers in neurology. 2019; 10:325. https://doi.org/10.3389/fneur.2019.00325 PMID: 31019487

121. Asher EE, Plotnik M, Gčnther M, Moshel S, Levy O, Havlin S, et al. Connectivity of EEG synchronization networks increases for Parkinson's disease patients with freezing of gait. Communications biology. 2021; 4(1):1–10. https://doi.org/10.1038/s42003-021-02544-w PMID: 34462540

122. Riba J, Romero S, Grasa E, Mena E, Carrié I, Barbanoj MJ. Increased frontal and paralimbic activation following ayahuasca, the pan-Amazonian inebriant. Psychopharmacology. 2006; 186(1):93–98. https://doi.org/10.1007/s00213-006-0358-7 PMID: 16575552

123. de Araujo DB, Ribeiro S, Cecchi GA, Carvalho FM, Sanchez TA, Pinto JP, et al. Seeing with the eyes shut: Neural basis of enhanced imagery following ayahuasca ingestion. Human brain mapping. 2012; 33(11):2550–2560. https://doi.org/10.1002/hbm.21381 PMID: 21922603

124. Dos Santos RG, Hallak JEC. Ayahuasca, an ancient substance with traditional and contemporary use in neuropsychiatry and neuroscience. Epilepsy & Behavior. 2021; 121:106300. https://doi.org/10.1016/j.yebeh.2019.04.053 PMID: 31182391

125. Aarsland D, Creese B, Politis M, Chaudhuri KR, Weintraub D, Ballard C, et al. Cognitive decline in Parkinson disease. Nature Reviews Neurology. 2017; 13(4):217–231. https://doi.org/10.1038/nrneurol.2017.27 PMID: 28257128

126. Smith R, Schöll M, Londos E, Ohlsson T, Hansson O. 18 F-AV-1451 in Parkinson's Disease with and without dementia and in Dementia with Lewy Bodies. Scientific reports. 2018; 8(1):1–6. https://doi.org/10.1038/s41598-018-23041-x PMID: 29549278

127. Rodriguez E, George N, Lachaux JP, Martinerie J, Renault B, Varela FJ. Perception's shadow: long-distance synchronization of human brain activity. Nature. 1999; 397(6718):430–433. https://doi.org/10.1038/17120 PMID: 9989408

128. Rubinov M, Sporns O. Complex network measures of brain connectivity: uses and interpretations. Neuroimage. 2010; 52(3):1059–1069. https://doi.org/10.1016/j.neuroimage.2009.10.003 PMID: 19819337

129. Cope TE, Rittman T, Borchert RJ, Jones PS, Vatansever D, Allinson K, et al. Tau burden and the functional connectome in Alzheimer's disease and progressive supranuclear palsy. Brain. 2018; 141 (2):550–567. https://doi.org/10.1093/brain/awx347 PMID: 29293892

130. Peraza LR, Díaz-Parra A, Kennion O, Moratal D, Taylor JP, Kaiser M, et al. Structural connectivity centrality changes mark the path toward Alzheimer's disease. Alzheimer's & Dementia: Diagnosis, Assessment & Disease Monitoring. 2019; 11:98–107. https://doi.org/10.1016/j.dadm.2018.12.004 PMID: 30723773

131. Ebadi A, Dalboni da Rocha JL, Nagaraju DB, Tovar-Moll F, Bramati I, Coutinho G, et al. Ensemble classification of Alzheimer's disease and mild cognitive impairment based on complex graph measures from diffusion tensor images. Frontiers in neuroscience. 2017; 11:56. https://doi.org/10.3389/fnins.2017.00056 PMID: 28293162

132. Pereira JB, Mijalkov M, Kakaei E, Mecocci P, Vellas B, Tsolaki M, et al. Disrupted network topology in patients with stable and progressive mild cognitive impairment and Alzheimer's disease. Cerebral Cortex. 2016; 26(8):3476–3493. https://doi.org/10.1093/cercor/bhw128 PMID: 27178195

133. Coninck JC, Ferrari FA, Reis AS, Iarosz KC, Caldas IL, Batista AM, et al. Network properties of healthy and Alzheimer brains. Physica A: Statistical Mechanics and its Applications. 2020; 547:124475. https://doi.org/10.1016/j.physa.2020.124475

134. Luo Y, Sun T, Ma C, Zhang X, Ji Y, Fu X, et al. Alterations of Brain Networks in Alzheimer's Disease and Mild Cognitive Impairment: A Resting State fMRI Study Based on a Population-specific Brain Template. Neuroscience. 2021; 452:192–207. https://doi.org/10.1016/j.neuroscience.2020.10.023 PMID: 33197505

135. Viol A, Palhano-Fontes F, Onias H, de Araujo DB, Viswanathan G. Shannon entropy of brain functional complex networks under the influence of the psychedelic Ayahuasca. Scientific reports. 2017; 7(1):1–13. https://doi.org/10.1038/s41598-017-06854-0 PMID: 28785066

136. Tononi G, Sporns O, Edelman GM. A measure for brain complexity: relating functional segregation and integration in the nervous system. Proceedings of the National Academy of Sciences. 1994; 91 (11):5033–5037. https://doi.org/10.1073/pnas.91.11.5033 PMID: 8197179

137. Sporns O. Network analysis, complexity, and brain function. Complexity. 2002; 8(1):56–60. https://doi.org/10.1002/cplx.10047

138. Carhart-Harris RL, Leech R, Hellyer PJ, Shanahan M, Feilding A, Tagliazucchi E, et al. The entropic brain: a theory of conscious states informed by neuroimaging research with psychedelic drugs. Frontiers in human neuroscience. 2014; p. 20. https://doi.org/10.3389/fnhum.2014.00020 PMID: 24550805

139. Carhart-Harris RL. The entropic brain-revisited. Neuropharmacology. 2018; 142:167–178. https://doi.org/10.1016/j.neuropharm.2018.03.010 PMID: 29548884

140. Papo D. Commentary: The entropic brain: a theory of conscious states informed by neuroimaging research with psychedelic drugs. Frontiers in human neuroscience. 2016; p. 423. https://doi.org/10.3389/fnhum.2016.00423 PMID: 27624312

141. Pallavicini C, Cavanna F, Zamberlan F, de la Fuente LA, Arias M, Romero MC, et al. Neural and subjective effects of inhaled DMT in natural settings. bioRxiv. 2020;.